· Università degli Studi di Napoli Federico II

Dipartimento di Ingegneria Chimica, dei Materiali e della Produzione Industriale

Dottorato in Ingegneria dei Materiali e delle Strutture

Molecular simulations of biomolecules-inorganic interactions for hybrid material design

—

Tesi di dottorato
in Biomateriali

Advisor
Prof. Ing.
Paolo Antonio Netti
Prof. Ing.
Filippo Causa
Coordinatore
Prof. Ing.
Giuseppe Mensitieri

Presentata da
Chiara Cosenza

XXVI Ciclo

Contents

Chapter 1

Introduction and background

Recent advances in nanotechnology have focused the attention to novel physical and chemical properties typical of materials with a nanometer length. These features open up new possibilities for a wide range of technological applications. The observation of the matter deeper to the nanoscale, thank to powerful measurement techniques and the ability to operate at this length scale are the milestones of different innovative researches in the last decade. In biomaterial field an interesting aspect is building up biological-inorganic hybrid materials. The design at bio-inorganic interface is connected with nanomaterials synthesis, surface functionalization for relevant biomedical aspects such as regenerative medicine, nanostructures for electronic devices, highly sensible biosensors and diagnostic. Rational hybrid bio-inorganic design is a challenge since an accurate and exhaustive knowledge of the interactions at the interface is needed. Taking in mind all these different aspects, it has been studied the interaction between small protein sequences and noble metals. The protein sequences are referred as specific peptides for inorganics due to the fact that these sequences have an highly specific interaction for a target inorganic material. They have been selected thank to combinatorial selection molecular biology techniques that will be analyzed in the following parts. Indeed this research topic lays in the context of "Nanotechnology through Biology"[1] and it is clear this is an interdisciplinary one,

in which engineering, biology and chemistry features come together. Moreover, peptides for inorganic have been proved to serve as protective agents for metallic nanoparticle surfaces and stabilize them against the formation of aggregates.[2] To be able to handle with the bio-inorganic interfaces several experimental measurements have been adopted in the last decade, first of all adsorption quantification techniques.[3] Other experimental tools have been atomic force microscopy[4] for surface topography evaluation after the adsorption, conformational examination of proteins and surface charge measurements.

More the knowledge at the interface, more the possibility to develop new applications. To this aim, parallel to experimental activity, molecular simulation studies have been employed.[5, 6, 7, 8, 9, 10] Studying the mechanisms of interaction at the interfaces thank to molecular simulations in the context of the measurements, in an integrated approach, provides a complete vision of the interaction, as proposed in a very recent work done by Tang et Al.[11] Molecular simulation overcomes the experimental limits, giving details till to atomic level. Softwares and simulation parameters have been developed by theoretical groups to the common purpose to better reproduce the bio-inorganic interface in water solution.[12, 13] Better this ability, better the consensus to this approach. After the whole validation of the theoretical parameters, experiments could be guided by simulation results, reducing the speculation in experimental activity and in this way the total research cost.

To this aim, in connection to the experimental part, it has been studied from a theoretical point view the interaction of a peptide sequence, named AuΦ3, with the gold substrate.[14] The activity has used molecular dynamics simulation and proper methods of data analysis to reveal different informations you can obtain from this kind of approach. Several aspects have been investigated to this purpose: the dynamics of the peptide during the binding event, the interacting parts, the conformations assumed in solution and at the interface, the binding energy and the entropic loss during the adsorption

event. The data have been compared with experimental and *in silico* results regarding gold binding peptides selected by other groups. This approach has employed parameters[12, 15] proper to describe a system in which there are both biomolecules and inorganic species in a water solution environment. Moreover in the light of the gained results it has been proposed a scheme to conjugate the AuΦ3 sequence with other molecular entities to promote the gold surface bio-activation. Other molecular simulations are carried on to explore the effects of the conjugation on adsorption.

In the first chapter, a general introduction to the research regarding bio-inorganic interactions and hybrid material design is provided. It also includes possible applications as discussed in current research works, experimental and theoretical approaches and critical issues. In the second chapter, the methods we employed for the simulation of biomolecules on gold surface are described in depth. In the third chapter, the achieved data are reported and widely discussed.

1.1 Peptides for inorganics

In nature proteins drive the precipitation of the inorganic fraction to form nanoparticles or materials with a well defined nanostructures. Following this natural evidence researchers have selected small protein sequences namely peptides, via combinatorial techniques, able to specifically interact with an inorganic substrate. Peptides are polymeric biomolecules, composed of amino-acids, with recognition capabilities that undergo distinctive sequence-specific self-assembly.[16] These features make them useful as building blocks for directing the growth and the assembly of nanostructures in a bottom up approach.[17] Peptides represent an alternative to chemical coupling to create functional nanostructures, i.e. materials that have at least one dimension within 1-100 nm length scale.[18] The size, the shape and the composition of the nanostructures strongly affect the optical, electrical and catalytic properties of the nanostructures and can be tuned to optimize their performance. Moreover, peptides can also act as morphology-control agents during the growth of nanomaterials in solution.[19]

1.1.1 Selection procedure and experimental characterization

The combinatorial techniques mostly adopted for this purpose have been the Phage display and the Cell Surface Display. The phage display is a molecular technology whereby peptides appear on the coat protein of a phage, a virus that infects a bacteria. A huge number of different peptide sequences (usually one billion of combinations) with a fixed length are displayed in a random pool of phage library as in fig.1.1a. This approach has been employed to select peptides that bind to solid inorganic materials using the biopanning procedure described in fig.1.1b.

The biopanning cycles aim to obtain only the peptide sequences that selectively bind to a desired substrate with high specificity. The biopanning

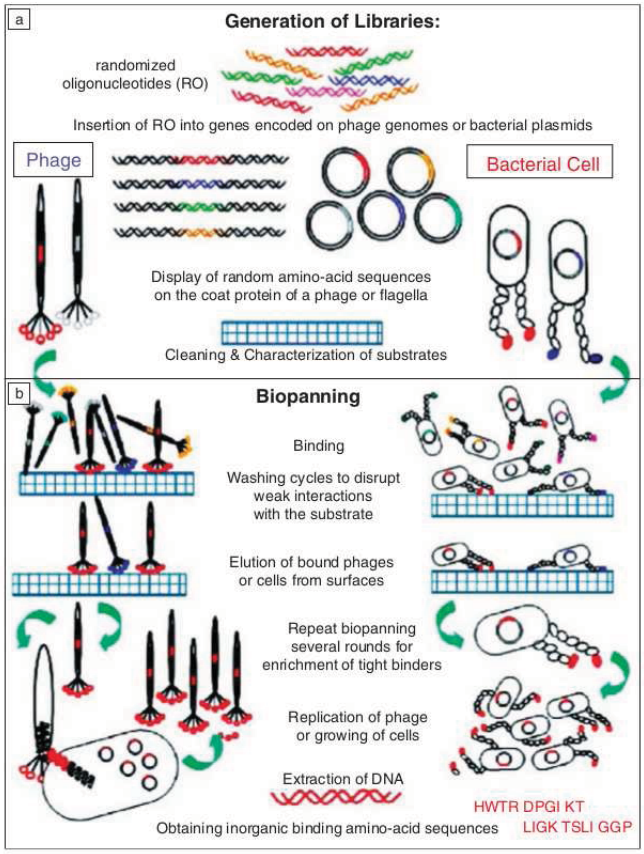

Figure 1.1: a) Combinatorial library construction and b) biopanning cycles in Phage Display selection. From Tamerler et al. 2008[20]

procedure consists in three steps, in the first one the phages exhibiting the different sequences are put in contact with the target substrate (binding step), then in the second step there are several washing cycles to remove the phages weakly bound to the substrate, finally the third step consists in the elution of bound phages from the surface. At the end of multiple biopanning cycles the phages are amplified and the amino-acid sequences are decoded obtaining the possible inorganic-binding peptides. Following this combinatorial selection technique peptides 8-12 amino-acids long have been selected against relevant technological inorganic materials. The investigated substrates have been noble metals such as Gold,[21, 22, 23, 24] Palladium[25]

and Silver[26] and metal-oxides[27, 28, 29, 30, 31] such as TiO_2 and Cu_2O. At the end of the selection procedure the ability to bind to the substrate have been proved both inside and outside the phage context. To this aim the binding characterization of phages exposing the inorganic-binding sequences has employed adsorption measurement techniques, above all the quantification of the bounded mass via the gravimetric test through the Quartz Crystal Microbalance (QCM)[32]. This test measures the change in frequency of a quartz crystal (a piezoelectric material), covered by the inorganic target material (such as gold), due to the adsorbed mass. Moreover it is possible to obtain the percentage of area covered by the adsorbed molecules. Adsorption isotherms have been obtained for both peptides displayed in the phage and *de novo* synthesized. Another technique widely used to test the adsorption of the inorganic-binding sequences has been the Surface Plasmon Resonance[3]. The mechanism of detection is based on that the adsorbing molecules cause changes in the local index of refraction, changing the resonance conditions of the surface plasmon waves inducing a shift in the signal that through data fitting procedures can be translated in useful kinetic and thermodynamic parameters.

1.2 Applications

1.2.1 Fabrication and assembly at nanoscale

A general and exaustive scheme of peptide for inorganics conjugation has been reported in the scheme in fig.1.2 as proposed by Sarikaya et al. 2003.[1] In this scheme inorganic-binding peptides could be used as linkers for nanoparticle immobilization, as functional molecules assembled on specific substrates and as hetero-bifunctional linkers involving two (or more) binding proteins linking several nanoinorganic units. In a very recent work[33] silica binding peptides and gold binding peptides were fused together to form hybrid peptides. These designed fusion peptides enabled assembly of gold nanopar-

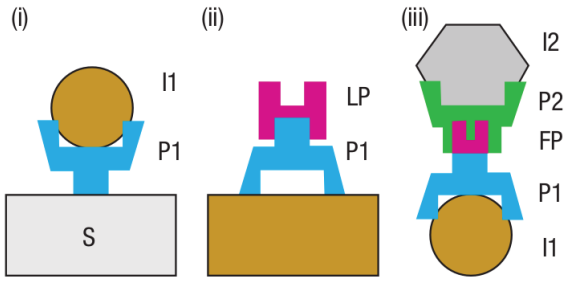

Figure 1.2: Peptides for inorganic conjugation as proprosed from Sarikaya et al. 2003[1] (I1:inorganic-1, I2:Inorganic-2, P1 and P2:inorganic specific proteins, LP:linker protein, FP:fusion protein)

ticles on silica surface producing a tool for nano-hybrid assembly as showed in fig.1.3.

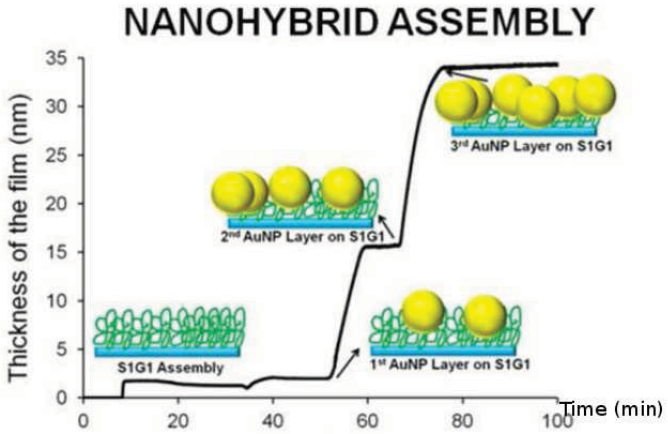

Figure 1.3: Assembly of the gold nanoparticles on a hybrid peptide decorated silica surface, as proprosed from Seker et al. 2014[33]

Hnilova et al.[34] also reported the controlled nano-fabrication of patterned gold film via modular multi-functional inorganic-binding peptides. They employed gold and silica binding peptide sequences, fused into a single molecule via a structural spacer, to assemble pre-synthesized gold nanoparticles on silica surface as showed in figure 1.4. Nochomovitz et al.[35] also provided another example of dual-affinity peptides for nanoparticles deposition and patterning on solid surfaces. Short binding peptides can also control and

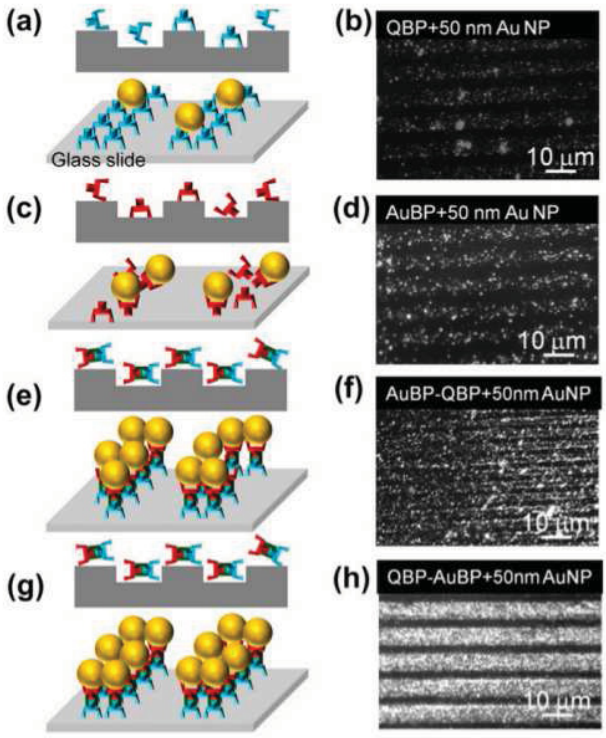

Figure 1.4: Efficiency of peptide-mediated gold nanoparticle immobilization. Schematics of peptide-mediated immobilization of gold nanoparticles using single or multi- functional peptides (a, c, e and g); respective dark field microscopy images of immobilized gold nanoparticles via QBP (b), AuBP (d), multi-functional AuBP–QBP (f) and QBP–AuBP permutations (h). From Hnilova et al. 2012[34]

enhance the protein immobilization onto specific solid surfaces in a botton up approach leading to the fabrication of hierarchical hybrid structures.[36]

Peptides for surface functionalization

In tissue engineering control the interaction between synthetic materials and human tissues in implants is a challenge. Since the early years of cell culture, biomaterial interfaces have been endowed with adsorbed extra cellular matrix (ECM) proteins, such as fibronectin, vitronectin, laminin and collagen, to support the cells and present an instructive background to guide

their behavior.[37] This approach still remains popular owing to its simplicity, and it has been enriched by using more selective techniques such as self-assembling monolayers (SAMs) to generate a defined surface able to control the nature and the distribution of protein adsorption. However, because cells depend on specific proteins for anchorage and extra-cellular instruction, the composition of the adsorbed layer is a key factor in cell behavior. The required proteins, correctly presented, can stimulate a constructive cell response, enabling wound repair and tissue integration, while proteins in an unrecognizable state may indicate foreign materials to be isolated or removed. However, the complexity and the dynamic nature of the involved process strongly limit the control on protein adsorption and impair the long-term stability. Therefore, shorter amino acid sequences present in extracellular proteins have been screened, which proved to elicit analogous stimuli with the advantages of being more stable and much easier to conjugate on material surfaces. Among these sequences, RGD, YIGSR, IKVAV, LGTIPG, PDGSR, LRE, LRGDN and IKLLI from laminin, RGD and DGEA from collagen I and RGD, KQAGDV, REDV and PHSRN from fibronectin have been identified. Probably the most studied peptide is the integrin-binding sequence RGD alone or integrated in a more complex architecture. Today, a considerable variety of peptide sequences containing RGD with different intrinsic abilities to promote various cell responses are known. Different molecular architectures containing the RGD sequence demonstrate different affinities for integrins as determined by the flanking residues, conformation and accessibility towards integrins. Therefore, these observations lead to the general statement that, besides the chemical entity of the biochemical signal, it is the way it is presented at the cell– material interface that plays a central role in regulating the cell response. There are different approaches in which a bioactive sequence can be presented towards a cell, and the manner in which the peptide is immobilized on a surface can affect the peptide concentration, density, arrangement, conformation and accessibility. The methods

of immobilizing peptide moieties on material surfaces can be classified into physical and chemical. Physical methods involve the adsorption or precipitation onto solid material, while, in the chemical approach, the peptide is covalently bound to the materials; the former probably leading to inactive conformations, the latter to be specifically designed. The accessibility of the peptide depends upon the chemical-physical and the texture properties of the surface, which, in turn, can be affected by the procedure of peptide conjugation on the surface.

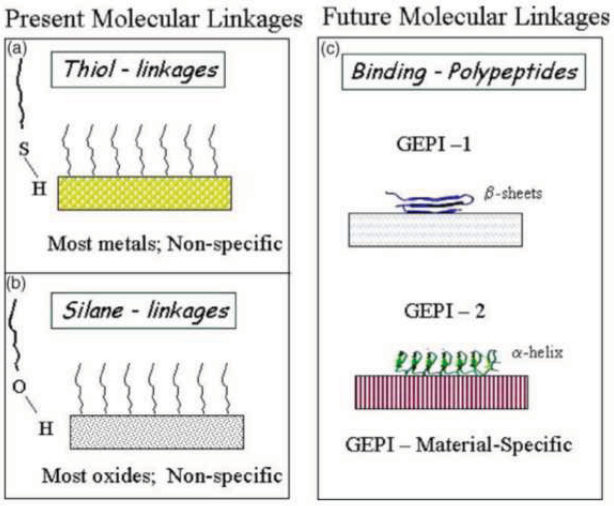

Figure 1.5: Comparison between SAMs and inorganic-binding peptides for surface functionalization. From Tamerler et al.[38]

The use of non covalent binding motifs, such as peptides for inorganics, could be a successful approach and an alternative to chemical coupling, they do not require any surface immobilization technique and they are highly specific for a target surface. Conversely self-assembled monolayer (SAM) linkages on metal inorganic surfaces, based on thiol or silane chemistry, have the disadvantage that SAM-surface interactions are nonspecific, as summarized in the schematic representation in fig.1.5 Two possible applications of inorganic-binding peptides, for surface functionalization, have been successfully reported by Sarikaya group in a paper published on *Acta biomaterialia*

in 2010.[39] In this study they have imparted cell-resistant properties to gold and platinum surfaces using specific peptides conjugated with poly(ethylene glycol) anti-fouling polymer. Moreover they have enhanced the cell-material interaction using peptides in conjunction with the integrin ligand RGD on glass and titanium surfaces, as reported in fig.1.6 a and b. The results indicate that control over the extent of cell–material interactions can be achieved by relatively simple and biocompatible surface modification procedures using inorganic binding peptides as linker molecules, as showed in fig.1.6 c and d[1]. Yazici et al.[40] provided another recent example for improving biologi-

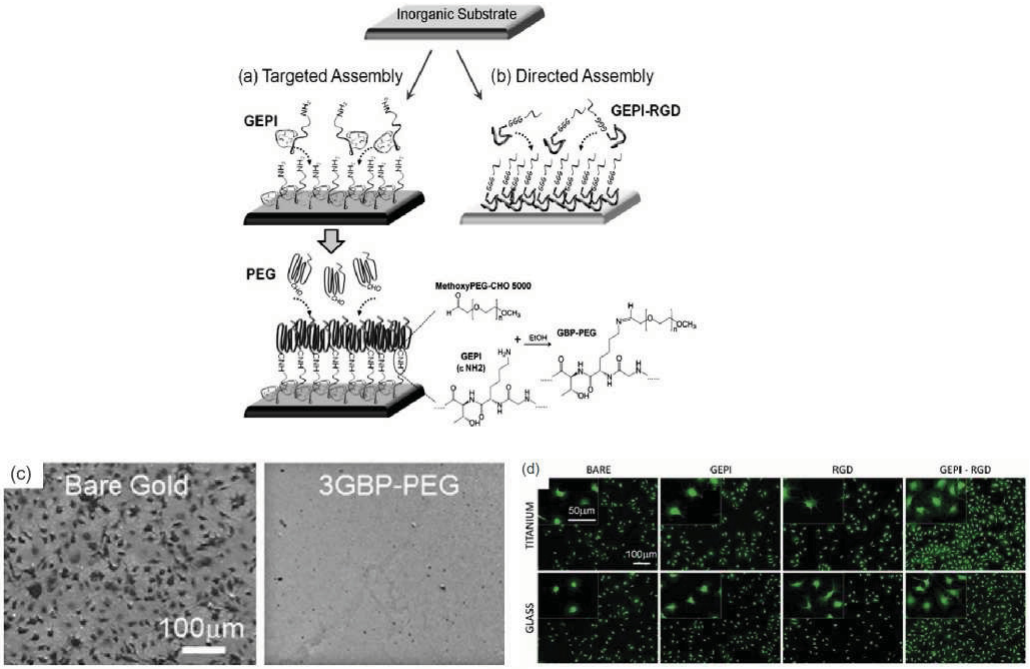

Figure 1.6: Surface functionalization for (a) anti-fouling and (b)cell-material interaction increase using Genetically Engineered Peptides for Inorganics (GEPI). (c) SEM micrographs of the bare and 3GBP1–PEG modified gold surfaces after 2 hours during cell adhesion experiments. (d) Fluorescence micrographs of cells on glass and titanium surfaces modified with RGD, GEPI and GEPI-RGD. From Khatayevich et al. 2010[39]

cal responses on the Ti-implant surface through the realization bi-functional

[1]3 GBP1 is a 14 mer specific peptide for gold isolated from Sarikaya group

peptides. They employed peptides, selected using a FliTrx cell surface display library, with different affinity for Titanium (Ti) surfaces. They firstly quantified the binding of the selected Titanium binding peptides (TiBP) via quartz crystal microbalance (QCM) and examined the cytotoxicity on Ti surfaces *in vitro*. Then the TiBP modularity was evaluated by conjugating them with an integrin recognition sequence, Arg–Gly–Asp–Ser (RGDS). It was demonstrated that the conjugated TiBP–RGDS not only retain their surface binding affinity, but also gain enhanced bioactivity to osteoblast and fibroblast cells, as confirmed by the following Fluorescence micrographs. Bio-enabled implant

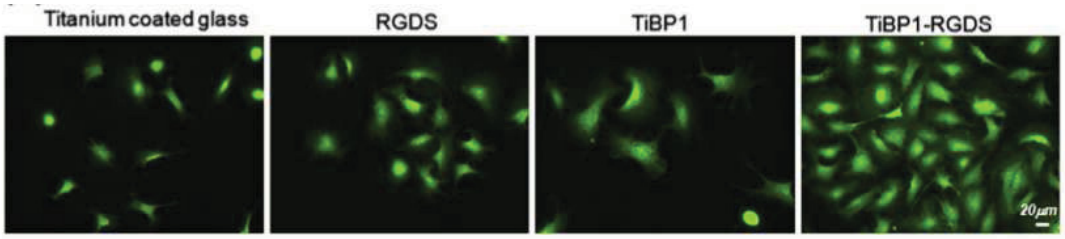

Figure 1.7: Fluorescence micrographs of cells on RGDS, TiBP1–RGDS-treated glass-coated Ti surfaces. Yazici et al. 2013[40]

surface functionalization using peptide-based linkers provides a platform for integrating the modular domains for multifunctional probe attachment on the surfaces in a single-step process under biologically relevant environments.

Nanoparticles formation

Noble metals nanoparticles exhibit unique optical properties strongly dependent on their size, shape and aggregation. This peculiarity brought to the possibility to employ them as active surfaces for surface-enhanced Raman, for chemical or biological sensing and for diagnostic imagining. The use of biomolecules to direct the organization of metal nanoparticles (above all gold, but also silver and platinum nanoparticles) into specific multifunctional nanostructures offers a promising route for the rational design of new materi-

als with predefined properties. In 2002 Naik and coworkers reported a synthesis method of peptide mediated silver nanoparticles.[22] Later on in 2005 the group of Slocik[2] showed the ability of specific peptides to control the synthesis and the aggregation of gold nanoparticles, reducing the choloraurate in solution and yelding to small (<10 nm) monodispersed Au spheres, as confirmed by TEM micrographs. Peptide-mediated control of the size and shape of gold nanostructures can be substantially affected by changing the reaction conditions, including pH and the concentration of choloraurate. Alteration of these parameters was shown to result in the production of gold nanostructures of diverse shapes (nanoparticles, nanowires, nanoribbons, kite and tail structures and nanometer thick platelets) and sizes (from a few nanometers to close to 100 μm).[41] In a very recent work Li et al.[42] employed twelve inorganic-binding peptides, with different affinity for gold, in the production of Au nanoparticles via a previously developed[25] reducing approach. The gold nanostructeres exhibited similar nanoparticle sizes, as proved in fig.1.8, but a different catalytic activity for the particular example of 4-nitrophenol reduction. In recent years, facet selectivity of peptide-metal adsorption has

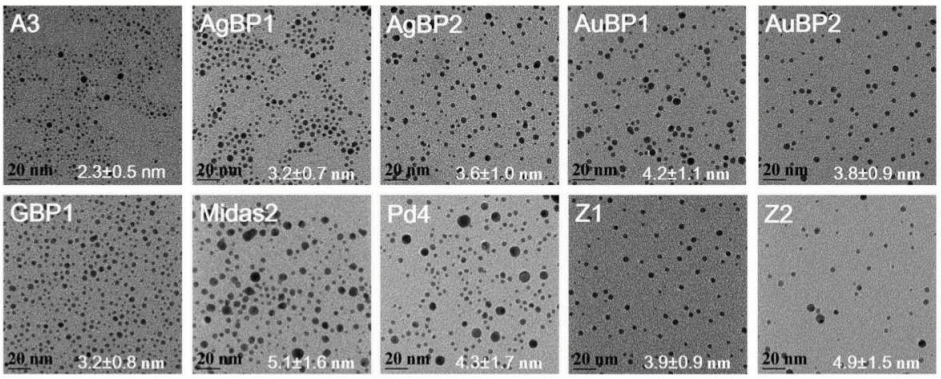

Figure 1.8: TEM analysis of Au nanoparticle formation mediated by twelve different inorganic binding peptides. From Li et al. 2014[42]

become of increasing interest to the biomimetic community. One goal of such work is to ultimately use biomolecules to exert fine control over metal

nanoparticles formation so that only nano-particles of a desired size and shape, targeted to specific application, are synthesized.[43] Recently, Huang and co workers realized this aim at the peptide-platinum interface, using peptides with high affinity specifically for either the Pt(100) or Pt(111) surface to synthesize platinum nano-particles (PtNPs) of different morphologies.[44]

Biomineralization-directing peptides

The Sarikaya group[45] reported the effects of two hydroxyapatite-binding heptapeptides, selected from Phage Display, on the mineralization of calcium phosphate mineral. They showed the two sequences, with different affinity for hydroxyapatite (HA) and different secondary structure and conformational stability, exhibited different influences on the formation of the mineral phase *in vitro*. The ability to form well defined three-dimensional networks

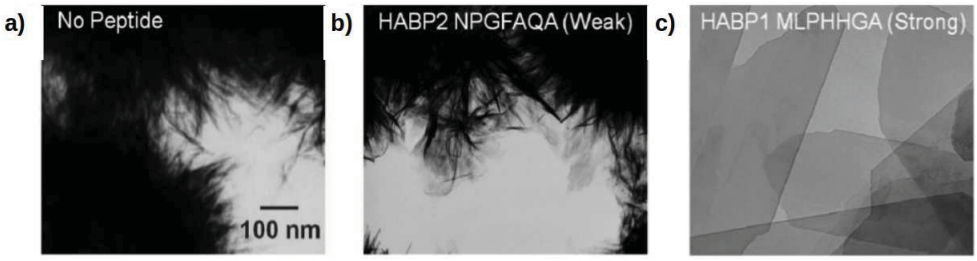

Figure 1.9: TEM images of the inorganic particles formed in the presence of: no binder (a), weak binder HABP2 (b), and strong binder HABP1 (c). From Gungormus et al. 2008[45]

that carry an inherent functionality makes these hybrid peptides attractive candidates for use in tissue engineering applications and ideal models for developing, multifunctional structures for nano-technological applications.

1.3 The AuΦ3 gold binding peptide and its applications

The AuΦ3 peptide is a gold binding peptide selected by Netti's research[14] group using combinatorial phage (M13) display technology. As in other works, the capability to bind to a gold surface has been proved after the selection procedure both inside and outside the hosting organism. Quartz cristal microbalance and Atomic Force Microscoy fig.1.10 have showed this capability in respect to the wild type (Wt) negative control (i.e. the phage without any sequence mutation). Moreover the adsorption selectivity against

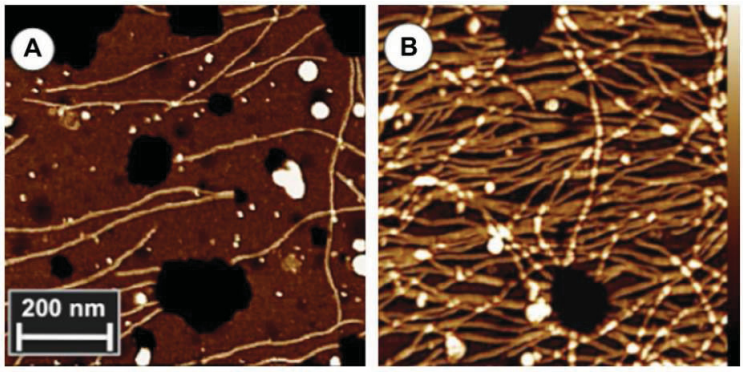

Figure 1.10: AFM images of Wt-M13 phages (A) and selected Au-PΦ3 phages (B) adsorbed on gold. From Causa et al. 2013[14]

different surfaces has been proved by Fluorescence images fig.1.11. Outside the phage context the binding behavior of linear peptide has been assessed by Surface Plasmon Resonance assay fig.1.12 with high affinity constant values ($K_{eq} = 10^6 M^{-1}$ and binding energies$= -8\ kcal/mol$) similar to other gold binding peptides. The the isothermal adsorption curves of SPR assays at different concentrations in fig.1.12 have been modeled through a bi-exponential fitting model as in other previous works regarding inorganic-bindind peptides.[3]

Steered Molecular Dynamics (SMD) and Molecular Dynamics have been per-

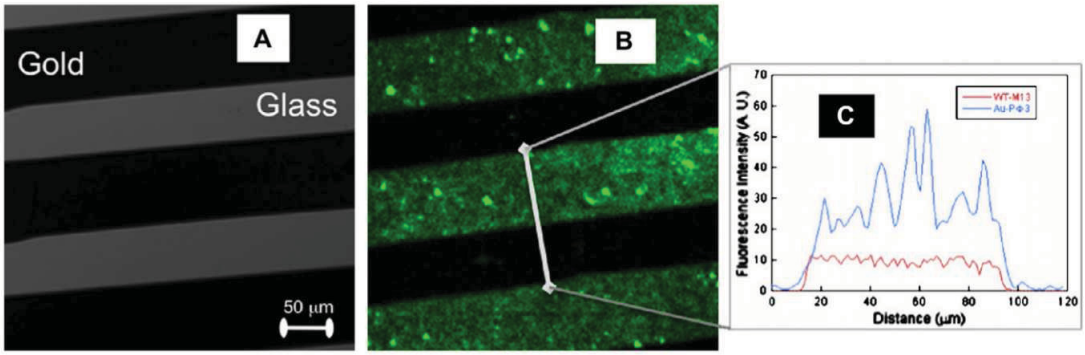

Figure 1.11: Selective Au-PΦ3 adsorption on gold: transmission (A) and fluorescence images (B) of Au-PΦ3 adsorbed on patterned micro-structure; (C) fluorescence intensity profile along gold stripe for Au-PΦ3 and Wt-M13 phage. From Causa et al. 2013[14]

formed to investigate the flexibility of the peptide in solution and in response to an applied force by comparing the AuΦ3 peptide with other sequences selected via the Phage-Display procedure. Through this preliminary *in silico* analysis the AuΦ3 peptide showed a lower flexibility in respect to the other sequences and for this reason the entropic contributions due to the adsorption seem to play a minor role. An accurate analysis of the entropic contributions will be described in the second chapter. The conformation of the peptide in solution was experimentally analyzed by Circular Dichroism spectra and a random coil structure for the AuΦ3 peptide in solution was determined. Recently, a method to use the AuΦ3 gold binding peptide has been proposed

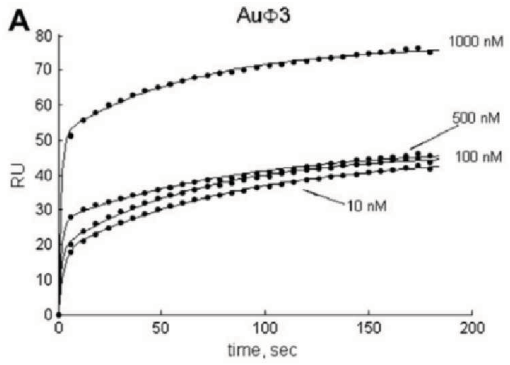

Figure 1.12: SPR analysis of peptides adsorption: adsorption isotherms for the peptide AuΦ3 obtained by SPR at different concentrations.From Causa et al. 2013[14]

for surface decoration of gold nanoparticles to induce SERS (Surface Enhanced Raman Spectroscopy) active surfaces.[46] They reported a method to direct and induce a reversible adsorption of the AuΦ3 peptide on gold, adjusting the ratio between gold nanoparticles and peptides in solution as showed by UV-vis spectra and TEM images in fig.1.13. Peptide mediated

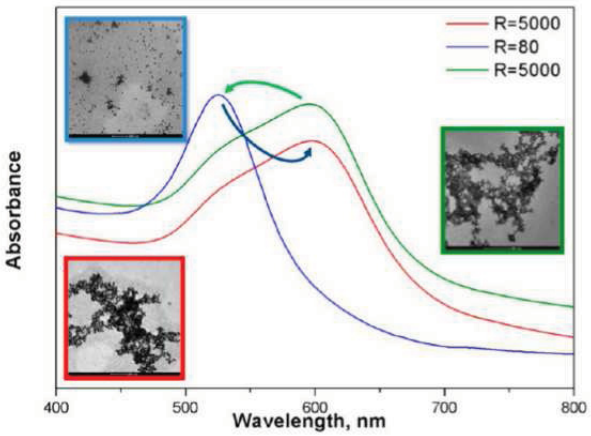

Figure 1.13: Different loading of AuΦ3 peptide in solution with gold nanoparticles exhibits a change in the U-vis absorption spectra. TEM micrographs in the insets show the reversibility of the aggregation process mediated by the AuΦ3 peptide. From Manikas et al. 2013[46]

gold nanoparticles assembly and disassembly lead to the formation of two

technological appealing materials: gold aggregates and single decorated gold nanoparticles. The former has proved to generate a SERS active substrate for the detection of very small-volume and low concentration samples as showed by the presence of the RAMAN shift in fig.1.14a. In the specific case this substrate has been used for the detection of the Adenine, not detectable at this very low concentration without the presence of the AuΦ3 in the gold nanoparticles solution. Moreover AuΦ3-biotinylated single decorated gold nanoparticles were used as a separation-fishing technique, to separate the Streptavidin from a protein bath, as assessed by the ELISA test in fig.1.14b.

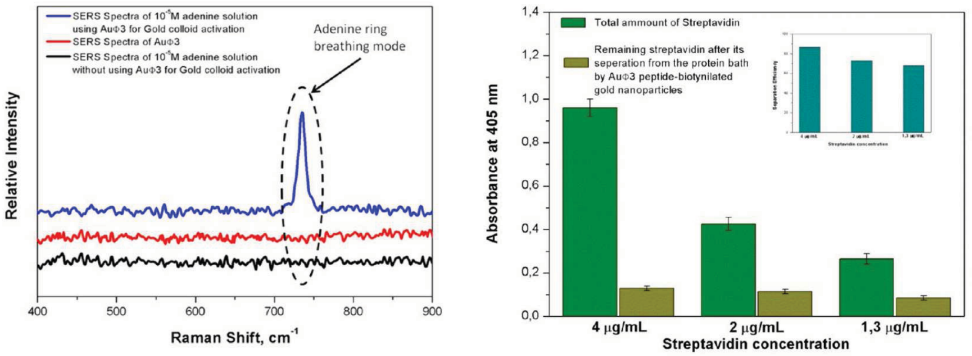

(a) (b)

Figure 1.14: a) SERS spectra of Adenine using AuΦ3 peptide for the gold nanoparticles aggregation-activation. b) ELISA tests confirmed the separation of Streptavidin from the protein bath using single-decorated gold nanoparticles. From Manikas et al. 2013[46]

1.4 Key parameters in peptides-inorganic interactions

1.4.1 Amino-acids identity

Understanding the basis of the interaction between combinatorially selected peptides and inorganic materials is crucial to furthering possible applications in many fields of nanotechnology. Using different experimental strategies, several authors have investigated the possible reasons for the high affinity of the selected chains. They mainly tried to quantify the propensity of each amino-acids to be adsorbed on a metal surface through the employment of homo-peptides i.e. chains of fixed length composed by the repetition of the same amino-acid. This way they tested the affinity of the 20 amino-acids against materials for technological applications. To this aim, Peelle et al.[24] conducted a systematic analysis of the peptide binding using yeast genetically engineered with six unit long homopeptides of all the 20 natural amino-acids against semiconductor and gold surfaces. They proved a differential adhesion among the homopeptides against the different target materials (fig.1.15) but it is worth noting they conducted their experiments in the contest of the hosting organism used during the biocombinatorial selection procedure. They found the Histidine homo-peptide was able to mediate binding of yeast to all the investigated surfaces, while the Methionine, Tryptophan and Cysteine homo-peptides exhibited different levels of binding to semiconductor and Au surfaces. They connected the binding ability of the homo-hexamers with the presence of residues containing side-chain functional groups with an aromatic secondary nitrogen (as in Histidine and Tryptophan) or a sulfur (as in Cysteine and Methionine). Other amino-acids (Glutamic Acid, Aspartic Acid, Tyrosine, Serine, Threonine, Lysine, and Arginine) were unable to confer binding as homopeptides within the systems they tested.
Willet et al.[47] have examined the adhesion of homopeptides *de novo* synthesized, 8 and 12 unit long, against several inorganic materials, finding that

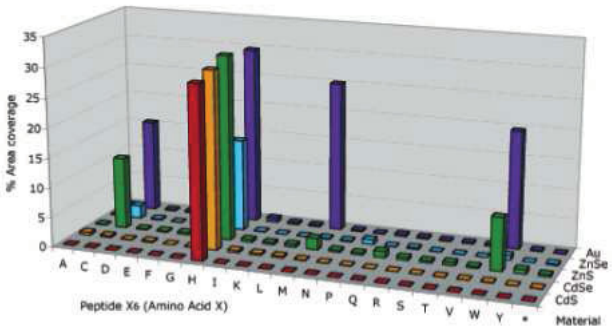

Figure 1.15: Differential adhesion of homopeptides against semiconductor and gold surfaces. From Peelle et al. 2005[24]

for the specific instance of gold surface Threonine and Arginine exhibited the greater adsorption. Conversely to experimental approaches, theoretical studies offered the possibility to quantify the adsorption strength of single amino-acids against a target surface. In the specific case of gold substrate, using molecular dynamics with different force-fields and different methods of calculation, Hoefling et al. (see fig.1.16a)[48] and Feng et al. (see fig.1.16a)[10] have established two affinity scales for all the amino-acids. Hoefling et al., employng the GoLP force-field[13], have showed the correlation between the chemical nature of the side chain amino-acids and their affinity against gold. Feng et al.,using the parameters of the CHARMM-METAL[12] force field (the same force field we have used in the present work), have found that large molecules with planar sp2 hybridizied groups adsorb most strongly. They also correlated the adsorption strength with the degree of coordination of polarizable atoms (O, N, C) to multiple epitaxial sites, introducing the concept of *soft epitaxy* for the adsorption phenomenon of peptides on metal surfaces. The main results of these two theoretical studies have been summarized in the following table. Both works present some similarities in the occurrence of some amino-acids as strong binders for gold. Both works identified Tyrosine, Triptophan, Methionine and Arginine as strong binders. There are also some similarities with the strong binding amino-acids exper-

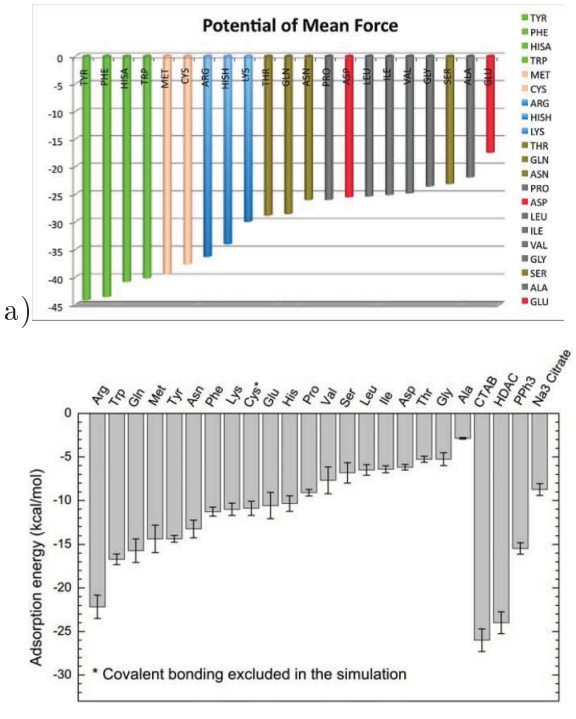

Figure 1.16: Amino-acids affinity scale as computed by a) Hoefling et al. 2010[48] (the values are the energy differences for each amino acid obtained from the Potential of Mean Force calculation in kJ/mol) and b) Feng et al.[10] (the values are adsorption energies from molecular dynamics calculation in kcal/mol)

imentally identified by Peelle (Methionine and Triptophan). The presence of strong affinity amino-acids plays a role in the interaction in terms of the enthalpic gain associated with the binding event but, as assessed in several studies, the mere presence of strong binding amino-acids doesn't necessary induce the high affinity of the whole chain.

1.4.2 Amino-acids sequence

The particular disposition of the amino-acids[28] in the chain can tune the ability of the sequence to be adsorbed. Peelle et al.[24] also tested the ability of the neighbors in the chain to up- and down-modulate the Histidine (the

Hoefling et al. 2010	Amino Acids
Strong Binding	Tyr, Phe, His, Trp, Met, Arg
Feng et al. 2011	Amino Acids
Strong Binding	Arg, Trp, Gln, Met, Tyr, Asn
Medium Binding	Phe, Lys, Cys, Glu, His, Pro
Low Binding	Val, Ser, Leu, Asp, Thr, Gly, Ala

Table 1.1: Amino-acids classification according to different theoretical calculations. In the calculation the contribution of covalent bonding is not considered.

strongest one) binding by use of interdigitated peptides (as XHXHXHX, in which X represents one of the 20 natural amino-acids and H is the one-letter code for Histidine). From these additional experiments they identified Glycine, Tyrosine, Glutamine, the basic residues (Lysine and Arginine) and the previous strong binding residues Histidine, Tryptophan, Cysteine and Methionine as up-modulating residues. The results of this experimental research, for the specific case of gold surface, has been summarized in the following table.

Peelle et al. 2005	Amino Acids
Strong Binding	His, Met, Trp, Cys
Up-modulating	His, Trp, Lys, Met, Cys, Arg, Gln, Tyr, Gly

Table 1.2: Strong binding and up-modulating amino-acids against gold surface according to Peelle et al. experiments.

1.4.3 Effect of sequence conformation

The conformation the chain assumes and the consecutive display of strong binder amino-acids has been discussed using both experimental and theoretical approaches.[49, 50] In this context, how the peptide molecular structure affects its recognition function is a fundamental question and it is still open. Hnilova et al.[23] have studied the effect of molecular conformation on the

binding behavior of FliTrx-selected gold-binding peptides *de novo* synthesized in linear and cyclic forms. They tested the adsorption of both the forms through surface plasmon resonance (SPR) spectroscopy and analyzed the adsorbed structure through circular dichroism and molecular mechanics studies. Recently, Corni et al.[51] studied the conformational behavior of the two gold-binding peptides and a control peptide that does not bind to gold. Firstly they confirmed, through SPR experiments, the higher adsorption of the two gold binding in respect to the control peptide although the three peptides possessed the same number of amino-acids previously identified as strong binder. They focused particular attention on the difference in flexibility of the chain both in solution and on the substrate. The two gold-binding peptides are highly flexible in solution but are able to adapt their conformation to the atomically flat gold surface. The control peptide, more rigid in solution, is not able to achieve a conformation able to allow all the strong binding amino-acids in the chain to contact with gold surface. The structures assumed by the flexible gold binding peptides on gold on one hand maximize the number of contacts between the amino-acids and the metal surface but on the other hand make the configurational entropic loss not negligible upon adsorption. Generally, all the peptides reduce the number of possible conformations during the adsorption but different inorganic-binding peptides loose different amount of conformations. To this aim in a very recent work Tang et al.[11] explored the conformational behavior of twelve different inorganic-binding peptides. They employed the cluster analysis to classify the conformations in groups like structure according to a geometrical rule, i.e. the difference in the root mean square deviations assumed by the backbone during the dynamics trajectories. Using this method they evaluated the different amount of entropy a peptide sequence can loose due to the adsorption. They assigned both enthalpic and entropic driving forces in the recognition process for all the twelve sequences they tested. A key aspect of their work is the possible connection of the conformations peptides can assume on the

surface and their possible applications mainly in surface modification and in nanostructures assembly.

1.5 Computational screening of biomolecules on inorganics

Molecular simulation techniques have been widely applied to several peptides or homo-peptides, using different conditions and methods, to explore the conformational behavior during the adsorption in solution on several inorganic surfaces.[5, 6, 52, 53, 54, 55, 44, 56, 57] Computational simulation of the aqueous peptide-gold interface overcomes the experimental limits and are commonly used to understand the mechanisms driving adsorption at an atomic level. To make possible these analyses computational chemistry groups have developed specific parameters able to characterize systems in which there are proteins in solution at a metallic interface. In 2008 Heinz[12] and in 2009 Iori[13] presented parameters proper to describe the interaction of biomolecules with gold surfaces. The parameters calculated by Heinz have been combined with the biomolecular force field CHARMM[58] merging into the CHARMM-METAL force field that can be easily integrated in broadly used softwares for molecular simulations like CHARMM[59] and NAMD[60].

In 2002 Braun et al.[61] studied the behavior of a 3-repeat gold binding peptide on different gold surfaces, Au(111) and Au(211). Later on Heinz et al.[62] studied the *in silico* adsorption of other peptides on gold, platinum and mixed gold-platinum surfaces. In 2010 Heinz[63] proposed and tested two methods to compute the change in energy, entropy and free energy upon adsorption of biomolecules on nanoscale surfaces, as illustrated in fig.1.17.
The first method involves the simulation of the adsorbate on the surface (simulation 1) and in solution (simulation 2) using the same box size and box content, fig.1.17a. The box needs to be large enough to avoid contact of the adsorbate with the surface during the solution run. However, large

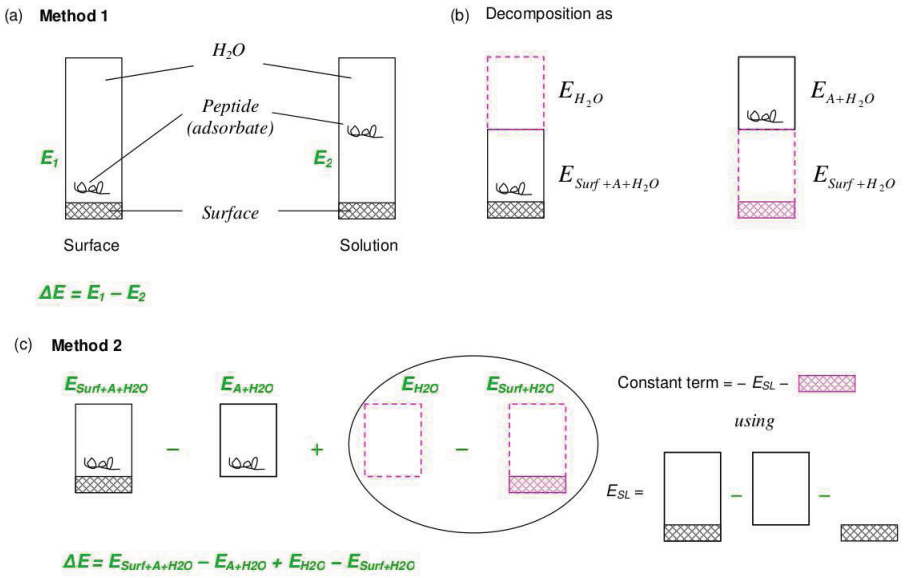

Figure 1.17: Computation of adsorption energies under periodic boundary conditions (illustrations in 2D for simplicity). (a) Method 1 involves the calculation of average energies in two simulation boxes with the adsorbate on the surface and in solution. (b) Decomposition into smaller boxes for reduced computation time and lower fluctuation in computed energy differences. (c) Method 2 involves four smaller boxes and is more efficient than method 1, particularly for screening many molecules on the same surface. From Heinz et al. 2010[63]

boxes result in high values and large fluctuations of the total energy which require extra simulation time to compute the relatively small energy difference $\Delta E = E_1 - E_2$ between simulation 1 and simulation 2 with statistically acceptable errors. The second methods consists in the decomposition of the two boxes in the method 1 in smaller four boxes. The calculations with smaller boxes are required which is approximately twice as fast as two calculations with larger boxes using Ewald procedures or spherical cutoffs for Lennard-Jones interactions. For computational screening of additional adsorbates on the same surface, only two additional calculations per adsorbate are required to obtain $E_{Surf+A+H2O}$ and E_{A+H2O} while the values for E_{H2O} and $_{EA+H2O}$ remain the same. The second method is useful for molecular screening of

different adsorbates on the same surface. A further advantage of method 2 over method 1 is the reduction of the total energy and its standard deviation, which lowers the standard deviation of computed adsorption energies on an absolute scale. Possible interferences from the surface in the solution run in method 1 are also eliminated, and method 2 equally provides access to thermodynamic quantities including energies, entropies, and free energies of adsorption. The application of either method, provided the box size is large enough to eliminate finite size effects and simulations are allowed to reach equilibrium, leads to identical results. Simulations are best performed using the NVT ensemble and additive molecular volumes, i.e., predefined densities for each constituent such as metal atoms, water molecules, and peptides. Then, for example, using the same cross section (A = xy) of the box, the box height (z) is incrementally additive for every component added. To compute differences in thermodynamic quantities, the simulation temperature must be constant or corrected to the same value using the heat capacity of each box (as derived in the simulation). Later on, as already discussed, Heinz's group has focused on the investigation of the specificity of single amino-acids on gold[10] with the aim to establish design rules for metal-binding biomolecules, based on the parameters of CHARMM-METAL force fiels. It is important to study the affinity of single amino-acids alone in order to construct an affinity scale of the single amino-acids but it is also important to study the interaction in context of the chain. The conformations assumed on the surface rely with the exposition of the high affinity groups. Furthermore, the influence of flexibility on binding was broadly discussed. Vila et al.[7] investigated the role of flexibility on adsorption comparing a multiple repeat of a gold-binding peptide and a non-gold binding peptide and later different homo-polypeptides[8] on gold surface. They addressed the higher flexibility as a propensity to the adsorption because it makes possible multiple conformation rearrangements of the peptides on gold. The effect of flexibility was also discussed by Yu et al.[64] As already mentioned, recently Corni et al.[51]

performed molecular dynamics simulation to investigate the conformational behavior of two gold-binding peptides with respect of a non gold-binding peptide. They widely discussed the effect of flexibility on molecular recognition properties giving an accurate quantification of the entropic effects during the adsorption based on the cluster analysis estimation. Recently Tang et al.[11] have proposed an integrated experimental and theoretical approach to elucidate enthalpic and entropic factors occurring during the binding events. They conducted a systematic analysis of twelve different metal binding peptides in order to clarify the reasons of the strong affinity against a particular surface. After an accurate comparison between the single amino-acids in the sequences and previous data from experimental and theoretical studies, they concluded that just the presence of strong binding amino-acids in a chain doesn't guarantee the strong affinity of the whole chain. This can be explained by the fact that during the binding event these amino-acids, due to the chain conformation, could not be in contact with the substrate. For this reason it has been necessary investigate the binding behavior of a particular sequence, in solution and in the presence of the substrate, also taking into account the conformation and the entropic factors. In general peptides lose entropy upon adsorption to a surface, but different sequences can lose different amount of entropy. For this reason they also quantified the entropic loss in term of the number of configurations assumed before and after the adsorption. They concluded that strong binding peptides from an entropic aspect are sequences assuming a different number of configurations on the surface. The previous works suggested that the interaction between peptides and metal surfaces is based not only on the presence of high affinity chemical groups in the peptide for the specific surface but also from the possibility of the peptide to assume different rearrangements on the surface, The Heinz's group has also presented two applications of the molecular simulation methods together with CHARMM-METAL ff, to investigate the influence of the shape of metal surfaces on adsorption[65] and another study to reveal the

specific crystallographic recognition of peptides and the resulting stabilization and size control of single-crystal NPs.[43] Yu et al.[66] also reported a molecular dynamics simulation study to reveal the stability-limited growth mechanism of peptide-mediated gold nanoparticles formation.

Taking in mind all the aspects exposed in these fundamental works we have studied the conformational behavior of a gold-binding dodecapetide previously selected through Phage Display.[14] We explored the possible conformations assumed in the adsorbed state via long molecular dynamics simulations at the aqueous-metal interface. We characterized the binding event from both enthalpic and entropic point of view always in the context of the whole chain. We assessed the most interactive and stable parts in the chain, the overall binding energy and the conformational entropic contribution upon adsorbed structures. Finally on the basis of the results we proposed a possible scheme of conjugation of the peptide with cell binding ligands to promote surface bio-activation. We further investigated two different conjugated peptides employing molecular dynamics and we highlighted the adsorption features among them.

Chapter 2

Methods

2.0.1 System construction

We employed molecular dynamics simulations to study the binding behavior of the gold-binding peptide AuΦ3 alone and in conjugation with cell binding ligands. The AuΦ3 peptide consists in 12 amino-acids: TLLVIRGLPGAC(T=Threonine, L=Leucine, V=Valine, I=Isoleucine, R=Arginine, G=Glycine, P=Proline, A=Alanine, C=Cysteine). We designed other two conjugated sequences in which two cell binding motifs are added to the amino terminus within the AuΦ3 original sequence. We chose two different cell binding motifs, the first one is composed by the amino-acid sequence RGD (Arginine-Glycine-Aspartic Acid) and the second one is the IKVAV (Isoleucine-Lysine-Valine-Alanine-Valine) sequence. For the RGD conjugation we also added one more Glycine and a Serine before and after the RGD respectively, as in previous experimental works[39]. The simulated sequences are reported in the following table 2.1.

Name	Sequences
AuΦ3	TLLVIRGLPGAC
GRGDS-AuΦ3	**GRGDS**TLLVIRGLPGAC
IKVAV-AuΦ3	**IKVAV**TLLVI1RGLPGAC

Table 2.1: The AuΦ3 and the conjugated sequences.

Since the NMR structures of the peptides are not available in the Protein Data Bank, on the basis of previous Circular Dichroism experiments[14], random coil structures of the sequences have been constructed using the Pro Builder online version at http://www.vegazz.net/. The peptides were modelled with the zwitterionic form of the N- and C- termini. All the sequences in the fully extended conformations were first equilibrated in a water box in NPT ensemble at 300 K and one atmosphere for 5 ns.

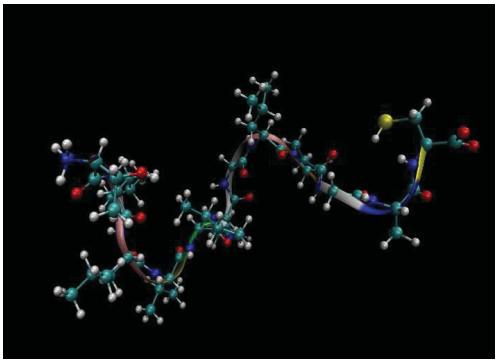

(a) AuΦ3

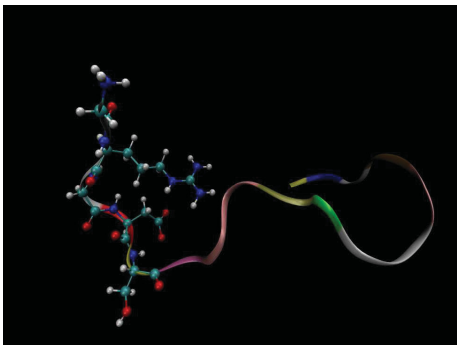

(b) GRGDS-AuΦ3

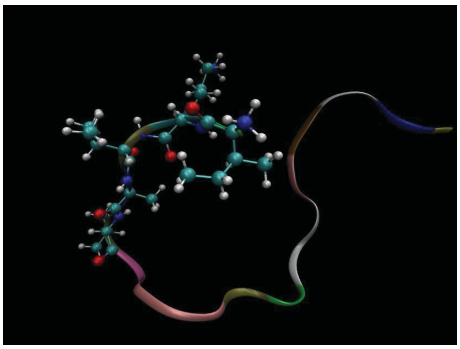

(c) IKVAV-AuΦ3

Figure 2.1: The AuΦ3 a) and conjugated peptides b) and c) at the end of the equilibration procedure. The backbone is reported in Ribbons representation and colored according to the residue names. In b) and c) the GRGDS and IKVAV cell binding motifs are highlighted in the CPK representation.

The final conformations of the equilibration procedure (fig.2.1) have been used as the starting structures for the production run simulations. In order to assess the rotational conformational sampling of the system six independent simulations were run. The starting configurations were generated rotating the peptide around the Head-Tail axis of 45 degree each. In fig.2.2 we reported the overlap of the rotated initial peptide configurations.

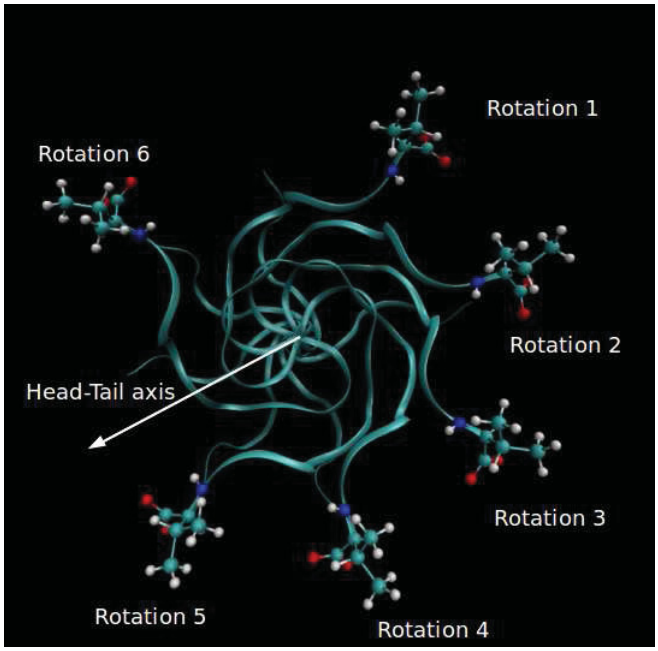

Figure 2.2: Rotational sampling representation: overlap of six initial rotated structures. The first residue is hilighted in the CPK representation, the backbone is in the Ribbons representation.

A gold surface of (81 x 81 x 20) Å was constructed using the Inorganic Builder module in VMD[67] from multiples of the unit cell of a Au{111} surface. The gold slab is composed by five layers. Then the peptide was placed with the center of mass at 20 Å above the top layer of the gold surface and the system was solvated using equilibrated water molecules through the VMD solvation package. In the simulation box were added ions in order to neutralize the solution. The simulation box was constructed in a way to avoid interactions

between the peptide and its nearest periodic image.

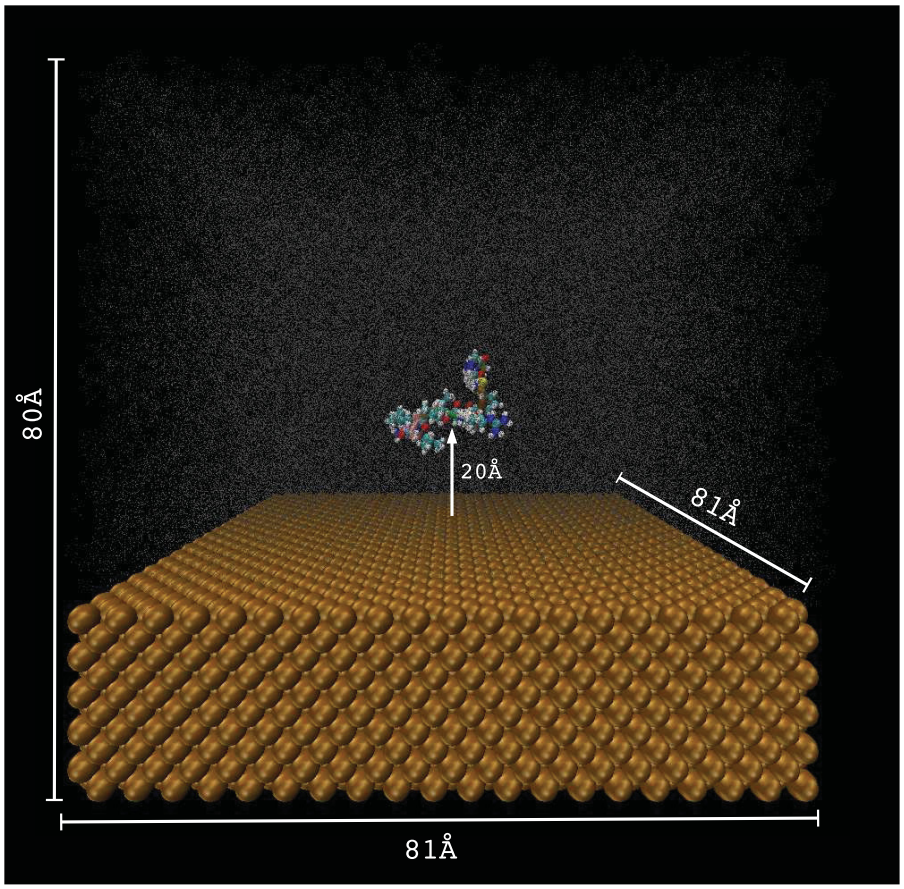

Figure 2.3: The simulation box with peptide, water and gold in a starting frame.

2.0.2 Simulation protocol

For the gold surface Lennard-Jones parametrization was used the CHARMM-Metal force field[12] and for the peptide CHARMM 22 force field.[58] Gold atoms were kept fixed during the simulations. For water molecules was adopted the TIP3 model. Starting from an equilibrated peptide configuration, the six simulations were performed in the NVT ensemble. We followed

the AuΦ3 dynamics till 100 ns and the conjugated AuΦ3 dynamics till 40 ns with 1 fs integration timestep. The NAMD package[60] was employed to perform the calculations. Simulations were carried on using periodic boundary conditions. The length and width of the periodic box were set to the size of the slab, so a continuous infinite gold slab was constructed. The system was first minimized using 800 steps of minimization to avoid bad contacts and to reduce the potential energy, then was heated at 300 K. During the production runs the Particle Mesh Ewald method was used with a grid spacing of 1 Å for Coulomb contributions. For van der Waals interactions the cutoff was set to 12 Å, with a smooth function between 10 and 12 Å. To keep the Temperature constant the Langevin Dynamics control was employed with a damping coefficient of 2/ps.

2.1 Analyzed quantities

We followed the dynamics of the peptide first in solution in a pure diffusive regime, then during the interaction with the metal substrate. From the trajectories of the system it is possible to gain informations about the conformation of the peptide in solution and on the metal surface, the binding energy and the entropic loss due to the adsorption.
All the trajectories have been firstly analyzed in the Visual Molecular Dynamics package (VMD)[67] and representative snapshots of the Auϕ3 and of the conjugated sequences adsorbed conformations have been taken, as in fig.2.4.

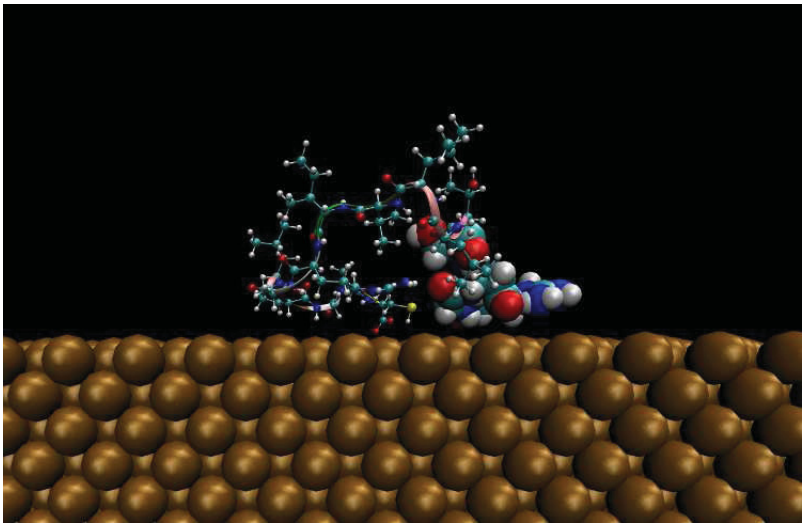

Figure 2.4: Snapshot of the GRGDS-Auϕ3 peptide on gold in a side view.

2.1.1 Dynamics of the interaction

To assess the interaction dynamics of each amino-acid during the adsorption event, the alpha carbons distances from the metal surface have been measured at several ranges of time. This analysis also allows to identify the various configurations of the peptides during the binding process as well as

at the equilibrium state after binding. The alpha-carbons coordinates have been extracted from the trajectories through TCL[1] scripting procedures in the TK console in VMD. The average has been computed over 1 ns of the trajectory simulation. Data elaboration and graphical representation have been performed using *ad hoc* scripting procedures in the MatLab©[2] environment.

2.1.2 Adsorption maps

To quantify the specific interaction of each amino-acid, adsorption maps have been constructed to represent the whole trajectory of the system according to a given threshold. As in previous studies[7] an amino-acid is considered adsorbed if the distance from the metal surface goes below 5 Å. The colored parts of the maps represent the amino-acids which have an average position of the alpha-carbons from the gold surface that goes below 5 Å. The average values have been computed over 1 ns of trajectory. In this way by the visual inspection of the adsorption maps is possible to understand which are the amino-acids taking part to the adsorption and if this event remains stable during all the simulation time. On the contrary, it is also possible to determine which amino-acids don't take part to the adsorption event. Through the analysis of the adsorption maps it is also possible to establish if there are parts of the chain preferentially adsorbed and parts that prefer to remain in solution. We also compiled a ranking of the amino-acids in the chain, based on the percentage time they are adsorbed during the simulations. The adsorption maps have been graphically elaborated in MatLab© through proper scripts.

2.1.3 Binding energy calculation

We also computed the binding energy E_B just for the Auϕ3 peptide as the difference between the energy of the whole system before and after

[1] Tool Command Language is a computer programming language
[2] MathWorks

binding.[63, 64, 66] We chose the Method 1 previously described in fig.1.17. Since the initial peptide's position was at a distance greater then the cutoff, we were able to calculate the energy of the system before binding E_0. The energy after binding E_1 can be computed at different times after the peptide started to interact with gold.

$$E_B = E_1 - E_0 \tag{2.1}$$

We considered the energy before binding, for each simulated system, the average energy value during the first nanosecond of simulation. We didn't compute the binding energies for one of the simulated systems because in this system the peptide started to adsorb during the first nanosecond of simulation and so we were not able to assess the energy before binding. In the determination of the average binding energy $\bar{E}_B$, for all the systems over the whole trajectory, we employed the block average method.[10] The simulation of the highest average value was discarded. The average binding energy (see equation 2.2) was computed using block averages of the two simulations of lowest average energies $\bar{E}_{B,2}$, the three simulations of lowest average energies $\bar{E}_{B,3}$ and the four simulations of lowest average energies $\bar{E}_{B,4}$.[10]

$$\bar{E}_B = (\bar{E}_{B,2} + \bar{E}_{B,3} + \bar{E}_{B,4})/3 \tag{2.2}$$

The uncertainty was calculated according to the following equation 2.3.

$$\Delta E_B = \pm(\left|\bar{E}_{B,4} - \bar{E}_{B,3}\right| + \left|\bar{E}_{B,4} - \bar{E}_{B,2}\right| + \left|\bar{E}_{B,3} - \bar{E}_{B,2}\right|) \tag{2.3}$$

These block averages reasonably represent the Boltzmann averages. The calculation has done skipping the initial minimization procedure, accounting for the total potential energy in the system. The data have been exported trough the NAMD Plot tool in VMD.

2.1.4 Cluster analysis

To assess the entropic loss of the Auϕ3 peptide above the surface, the conformations have been analyzed adding the Clustering[3] plugin to VMD. The plugin allows to calculate and visualize clusters of conformations for a simulation trajectory. The clusters are generated according to a geometric rule and it is also possible to decide how many clusters must be generated. In this way, it can be established how many frames belong to the same cluster and suitable informations regarding the entropic loss can be achieved in terms of the population number of each cluster on the surface during the adsorption. The conformations belonging to the same cluster are colored with the same color, as in the fig.2.5.

According to Tang et al.[11] the conformational ensemble generated from the dynamics trajectory at constant temperature was classified into groups of like structures on the basis of similarity of their backbone structures. A root-mean-squared deviation (RMSD) of 2 Å was chosen to generate the different clusters. The analysis was performed on the whole trajectory divided in 10 ns ranges of time, for the six simulated systems. We set the plugin to generate ten clusters of conformations. The population of a given cluster was calculated as the percentage fraction of the number of frames that were assigned membership of that cluster, divided by the total number of frames in the trajectory. To make a comparison with other simulations regarding metal binding peptides, we have classified the number of frames in a population according to the criteria proposed by Tang et al.[11] They established the criteria on the basis of the number of different possible arrangements of the peptide in the adsorbed state as a quantification of the conformational entropy of the adsorbed sequence. If a peptide assumes different adsorbed conformations the cluster analysis will not present highly populated clusters. On the contrary a peptide assuming just few adsorbed conformations will

[3] available at http://physiology.med.cornell.edu/faculty/hweinstein/vmdplugins/clustering/

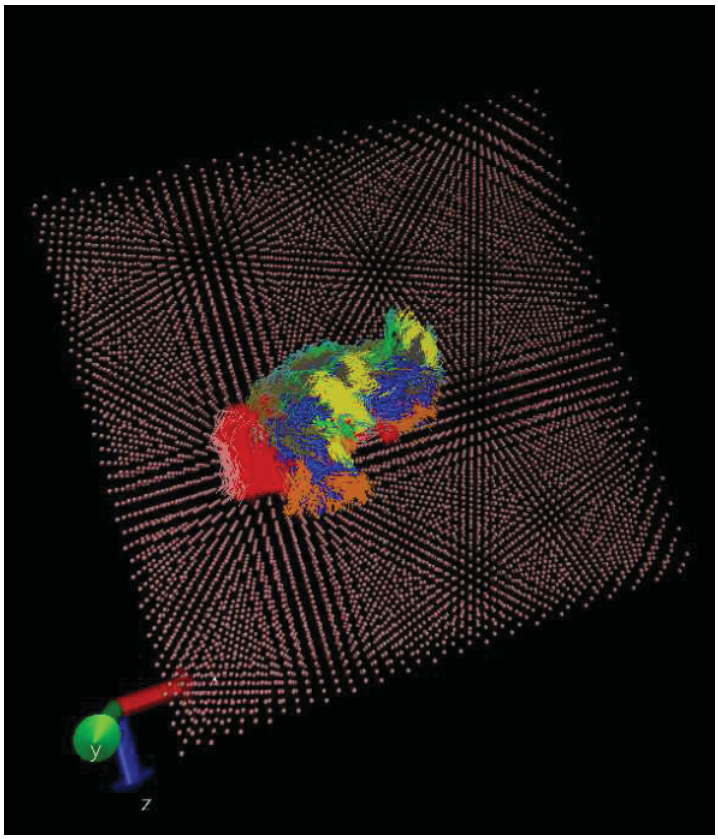

Figure 2.5: Snapshot of the cluster analysis for the Auϕ3 on the gold surface.

have highly populated clusters. They established that if the top 5 clusters have a population below the 60 % the entropic assignment to the binding peptide is high, i.e. the peptide is able to assume different adsorbed conformations. The entropic assignment must be low if the top 3 clusters have a population of the 75 %. The entropic assignment is medium in the other cases.

Chapter 3

Results and Discussion

3.1 AuΦ3 peptide

The binding affinity of a peptide to an inorganic surface is the result of a complex interplay between the binding strength of its individual residues and its conformation. Previous experimental and theoretical approaches widely discussed the need to address the binding affinity to the presence in the chain of highly strength residues and a favorable conformation assumed at the interface with the metal surface. To monitor interfaces at the nanometer scale and identify some of the underlying mechanisms of the bio-inorganic interactions molecular simulations can be a valuable tool.

In this work, we performed the theoretical investigation of the binding behavior of the AuΦ3 gold-binding peptide using classical molecular dynamics. We computed the trajectories of the system till to 100 ns, starting from different configurations. The system composed by the peptide in solution and in presence of the gold surface was modeled with specific force fields for the description of biomolecules and inorganic surfaces.

3.1.1 Adsorbed conformations

We monitored the simulation trajectories in time, taking representative snapshots of the AuΦ3 peptide during the adsorption event as in fig.3.1.

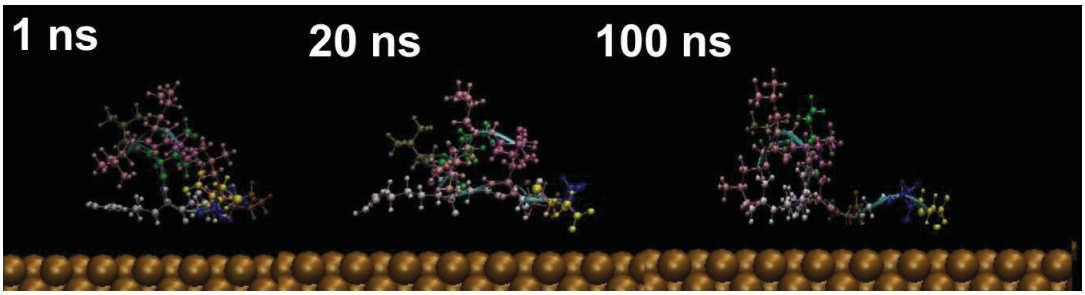

Figure 3.1: Multiple snapshots of the AuΦ3 peptide at different simulation times.

The visual inspection of the trajectories reveals a stability of the interaction during the simulation time. From a more accurate visualization we extracted the conformations mainly assumed by the AuΦ3 peptide above the gold surface. In fig.3.2a we reported the typical adsorbed conformation of the AuΦ3 peptide, in which it is clear there is a part mainly adsorbed on the surface and a part preferentially displayed in solution.

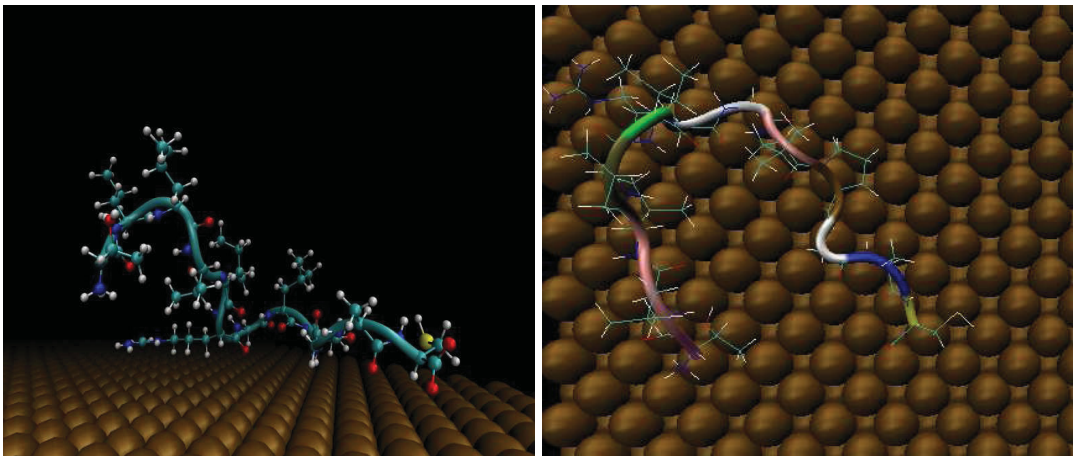

(a) side view (b) top view

Figure 3.2: Typical structures for the adsorbed conformations of the Auϕ3 peptide on gold.

3.1.2 Binding energies

The binding energy of the system, computed as the difference between the system before and after binding, confirmed an high affinity of the whole chain upon adsorption. The average binding energy E_B, computed using the block average method,[65] over five independent simulations for the whole trajectory gives a value of -200 $kcal\ mol^{-1}$ with an overall uncertainty around 20%. We also computed the average binding energies for the AuΦ3 at different time values and we made a comparison with the values relative to another binding peptide, A3, of the same length.[66]

times	5 ns	10ns	20ns
AuΦ3	-137	-130	-133
A3	-72	-89	-99

Table 3.1: Binding energies in comparison with other gold-binding peptides (values in $kcal\ mol^{-1}$)

3.1.3 Dynamics of the interaction upon adsorption

We reported the results regarding the dynamics of the six simulated systems, fig.3.3-3.8, in terms of the alpha-carbon average positions for several ranges of time: 10 ns, 20 ns, 50 ns and 100ns. At the beginning of the simulations the peptides were placed at a distance grater than the cutoff distance of the Au-peptide interactions and the time needed to approach the surface was controlled by a pure diffusive regime. After different amounts of simulation time, some residues started to interact with the gold surface as highlighted by the change in the peptide configurations. We assessed that in four simulated systems over six there is a common behavior in which the central part of the chain (Arginine 6 and Glycine 7) is the first interacting part. Then, as the simulation goes on, the tail (Cysteine 12 and Proline 10) reaches the surface. This configuration appears stationary for all the six simulated systems. On the contrary the head of chain resulted poorly interacting with the gold surface except for long simulation times and just for the first residue (Threonine 1). The equilibrium binding configurations resulted in a part preferentially adsorbed on gold and a part mainly displayed in solution.

Figure 3.3: Simulation 1 -Alpha-carbons distances (Å) starting at a reference angle of 0 degree.

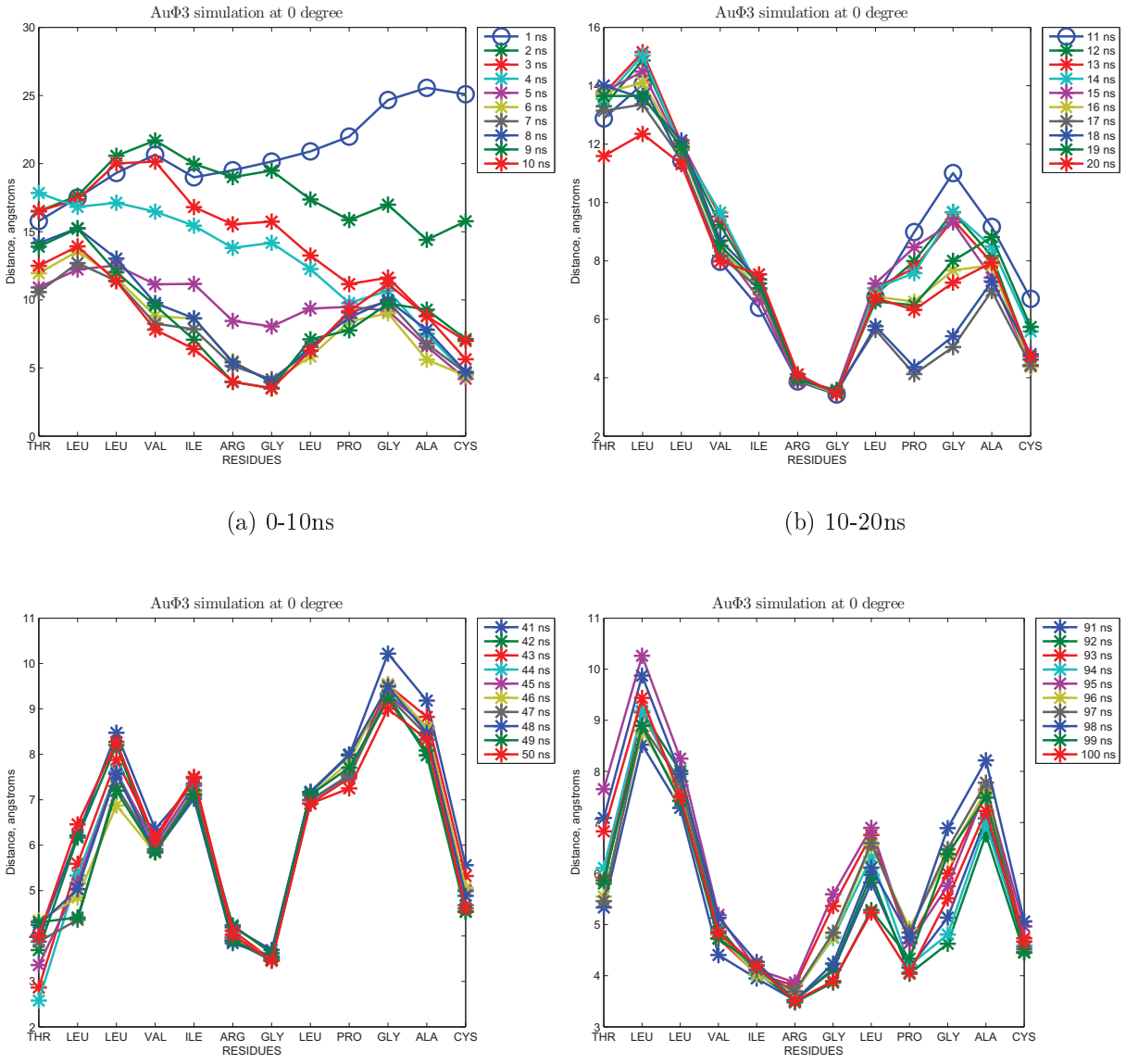

(a) 0-10ns

(b) 10-20ns

(c) 40-50ns

(d) 90-100ns

Figure 3.4: Simulation 2 -Alpha-carbons distances (Å) starting at a reference angle of 45 degree.

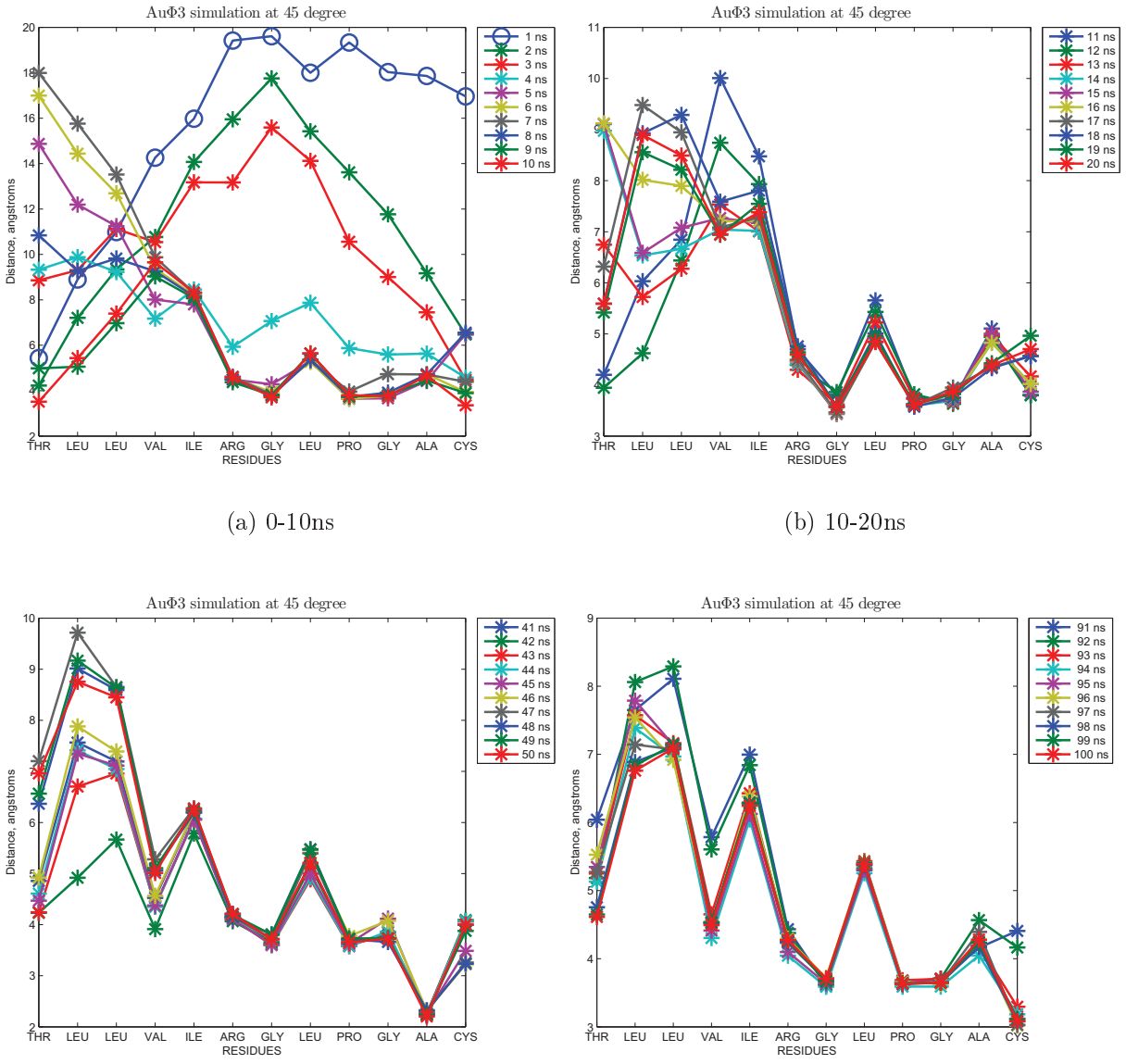

(a) 0-10ns

(b) 10-20ns

(c) 40-50ns

(d) 90-100ns

Figure 3.5: Simulation 3 -Alpha-carbons distances (Å) starting at a reference angle of 90 degree.

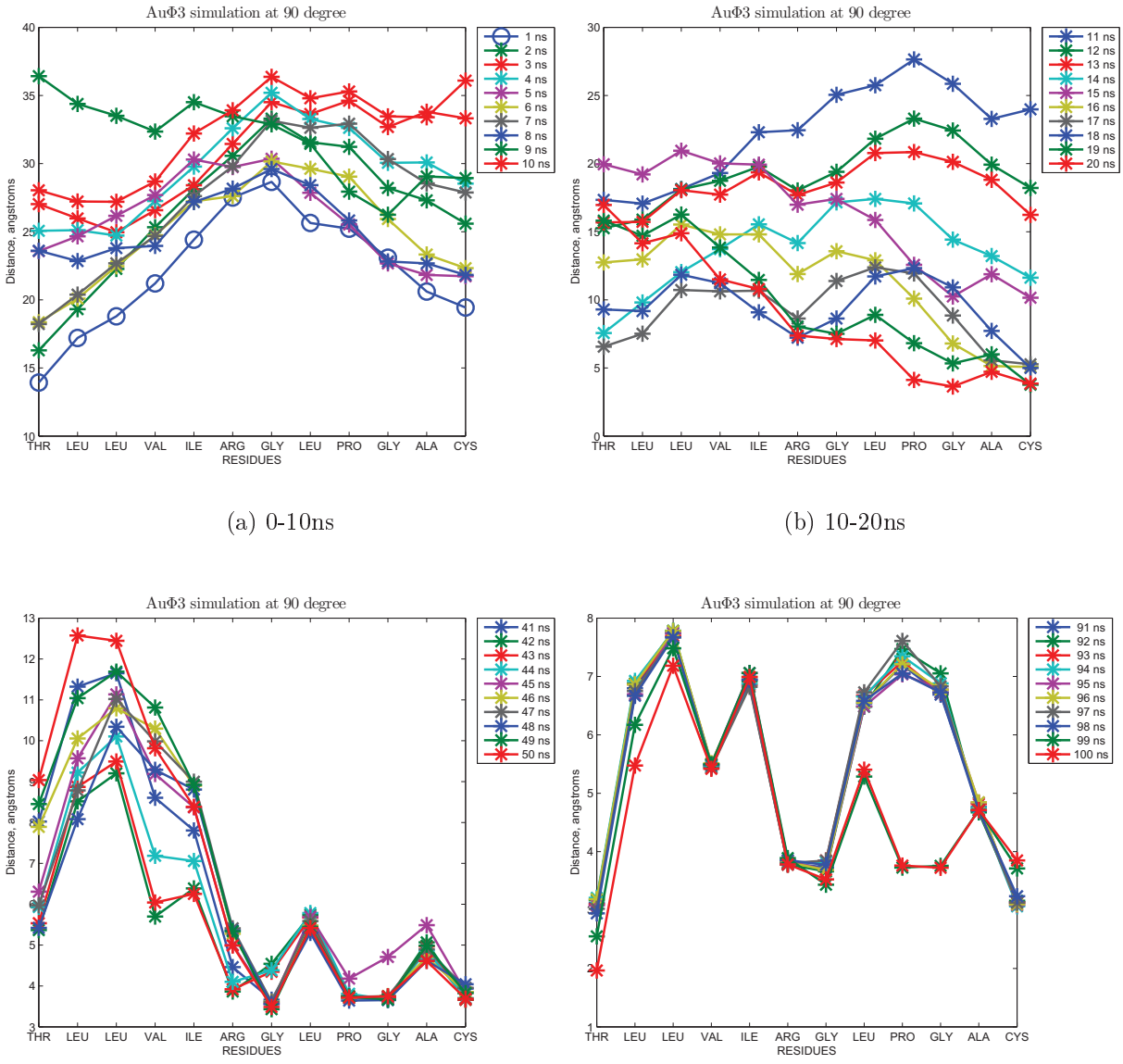

(a) 0-10ns

(b) 10-20ns

(c) 40-50ns

(d) 90-100ns

Figure 3.6: Simulation 4 -Alpha-carbons distances (Å) starting at a reference angle of 135 degree.

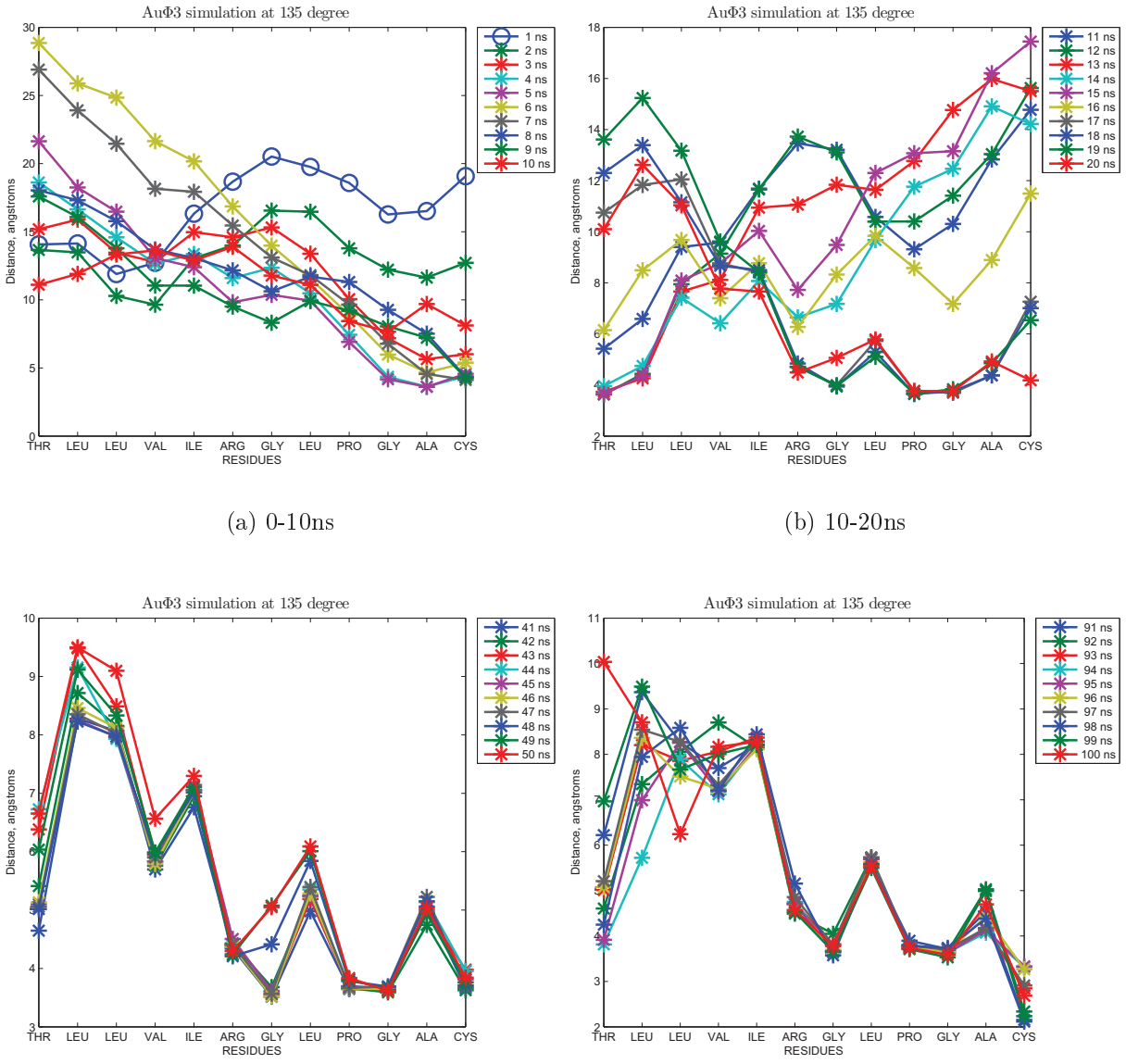

(a) 0-10ns

(b) 10-20ns

(c) 40-50ns

(d) 90-100ns

Figure 3.7: Simulation 5 -Alpha-carbons distances (Å) starting at a reference angle of 180 degree.

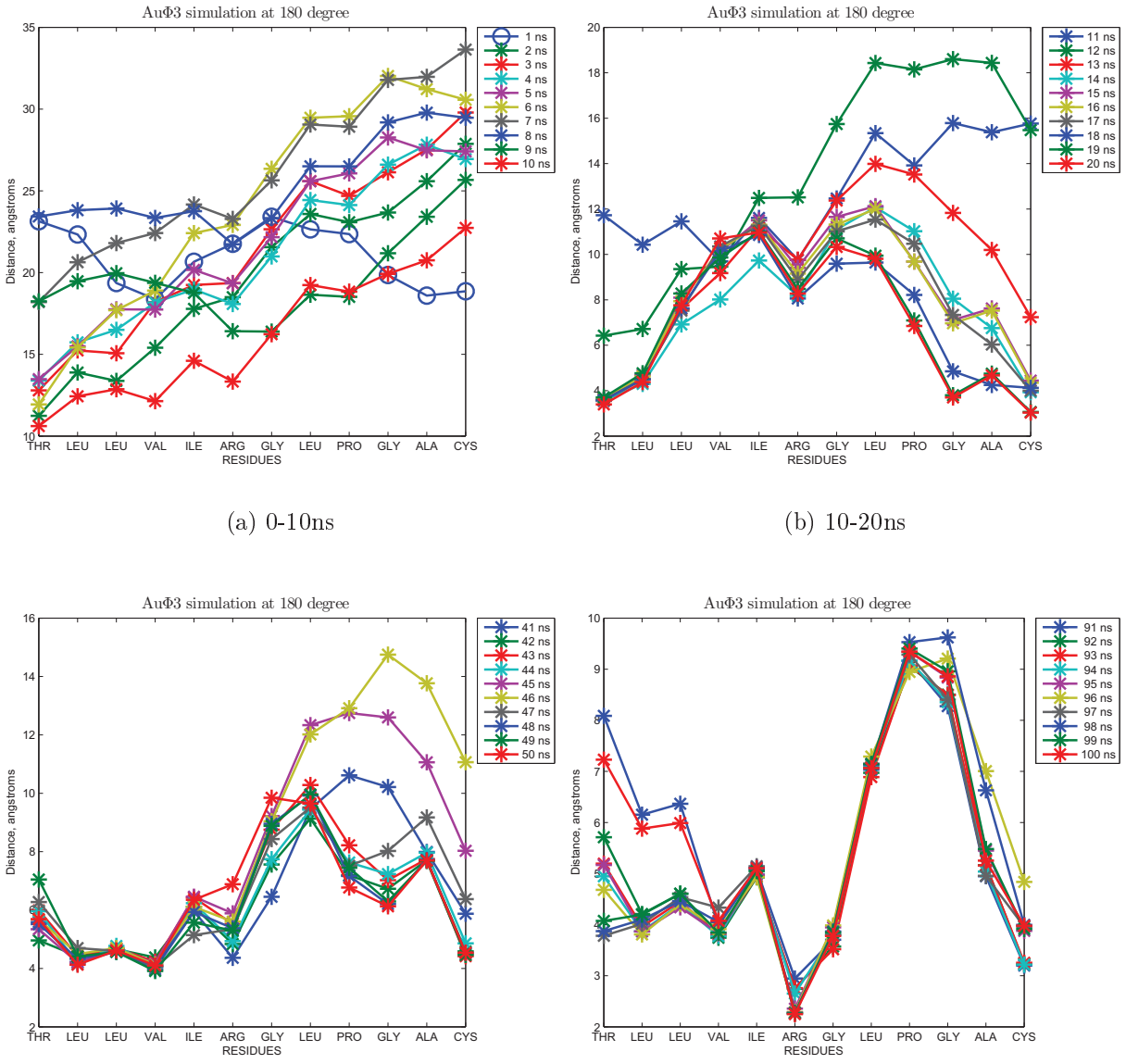

(a) 0-10ns

(b) 10-20ns

(c) 40-50ns

(d) 90-100ns

Figure 3.8: Simulation 6 -Alpha-carbons distances (Å) starting at a reference angle of 225 degree.

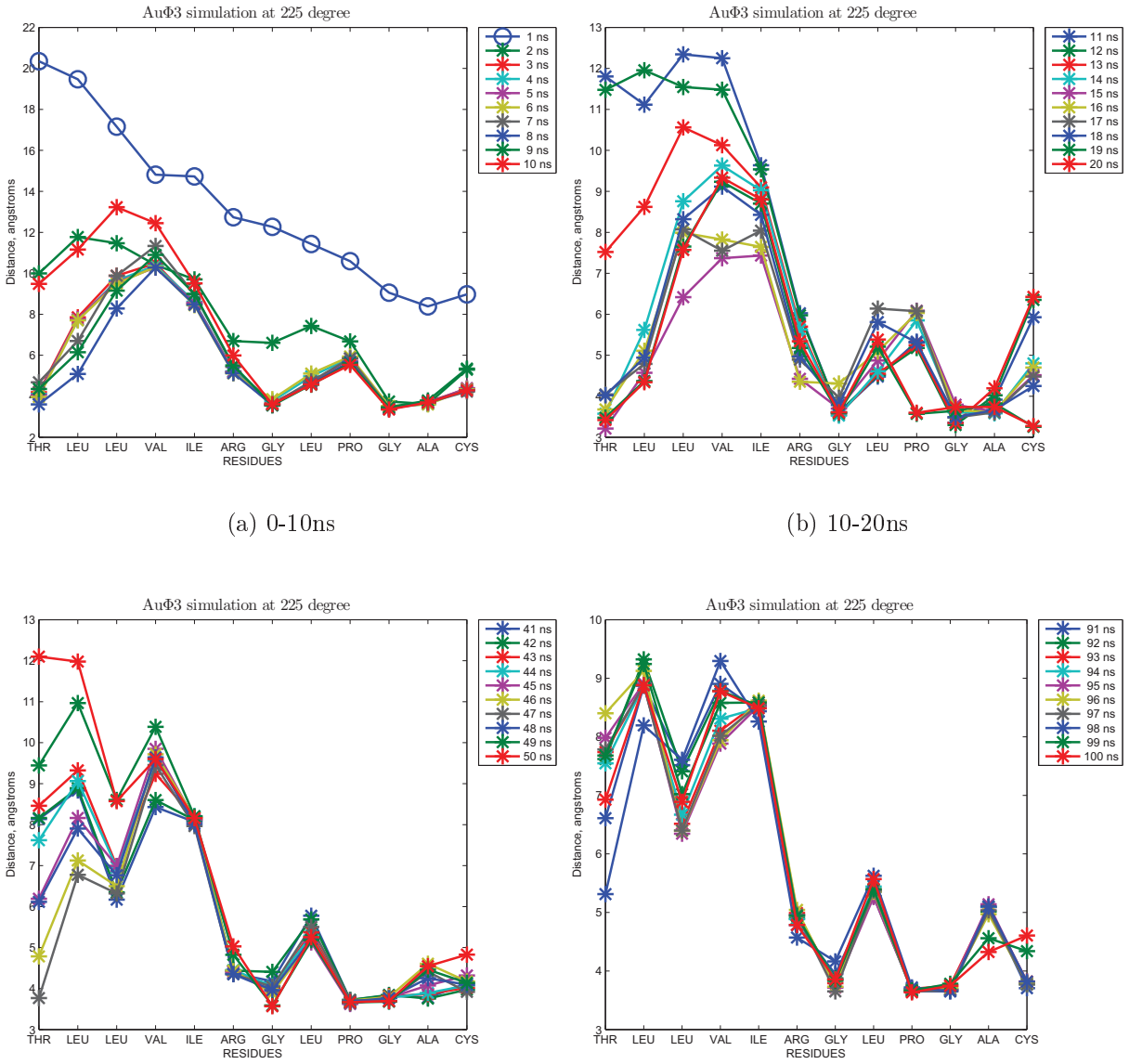

(a) 0-10ns

(b) 10-20ns

(c) 40-50ns

(d) 90-100ns

3.1.4 Adsorption parts

To better understand which are the amino-acids taking part during the adsorption and to monitor the adsorption in time, we also computed adsorption maps according to a given threshold. The adsorption maps for all the six simulated systems have been reported in fig.3.9.
The analysis of the adsorption maps assessed that the amino-acids taking part to the adsorption are: Arg6, Gly7, Pro9, Gly10, Ala11 and Cys12. In all the six simulated systems the adsorption of the Arginine and Cysteine remained stable in time for most of the trajectory. We expected the presence of Cysteine as a strong and permanent binding amino-acid. It is well known that experimentally Cysteine binds to gold via S-Au covalent bond. Conversely, the amino-acids Leu2, Leu3, Val4, Ile5 and Leu8 were less adsorbed. The first amino-acid the Threonine exhibited adsorption not stable during the simulation time. The adsorption scale for the amino-acids composing the Auϕ3 peptide, in terms of amount of time in which they are adsorbed, is reported in table 3.2.

rank	amino-acids	adsorbed time %
1	Cys12	82.5
2	Arg6	72.7
3	Gly7	70.0
4	Gly10	63.7
5	Pro9	61.5
6	Ala11	54.0
7	Thr1	28.7
8	Val4	23.0
9	Leu2	14.8
10	Leu3	8.17
11	Leu8	7.33
12	Ile5	5.5

Table 3.2: Frequency of occurence of adsorbed amino-acids

The role of the Arginine inside the sequence is crucial, as previously inden-

tified by Feng et al.[10] for single amino-acid simulations, from the visual inspection of the trajectory it is clear a near-perfect fit between the Arginine guanidium group and gold atoms. Moreover, we found Cysteine, Glycine and Proline highly involved in the interaction process. Furthermore, the trend for the less adsorbed amino-acids from our simulation matches with the table 1.1 identified by Feng et al.[10] for low binding amino-acids except that for the Glycines. Indeed in our simulations the Glycines are greatly adsorbed due to their high flexibility and because they are positioned next to strongly adsorbed amino-acids like Arginine and Proline.

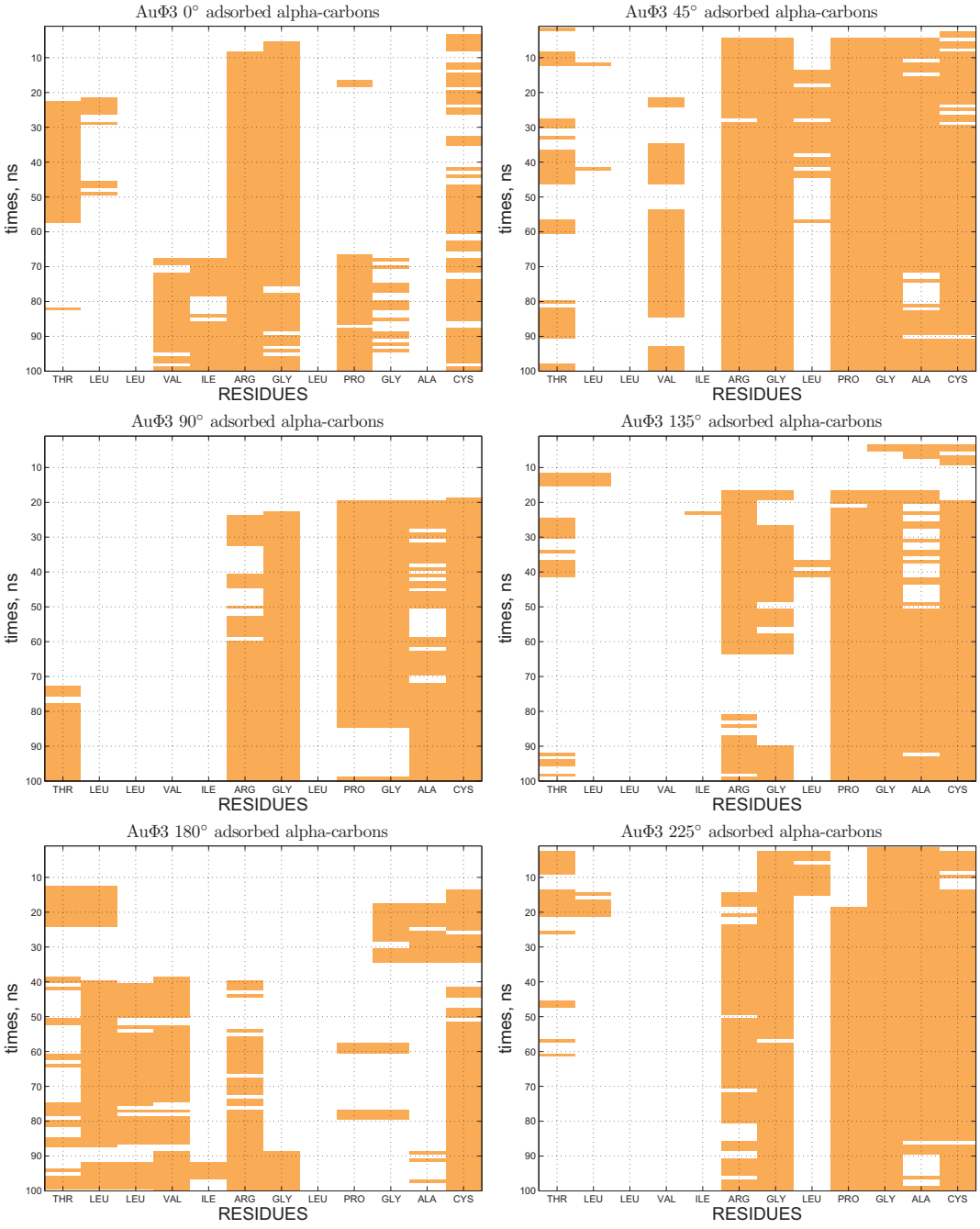

Figure 3.9: Adsorption maps of the alpha-carbons during the whole trajectory for the six simulations.

3.1.5 Entropic loss upon adsorption

After identify a general trend in the conformational behaviour of the sequence mainly composed by a strongly and a poorly adsorbed part, we performed an additional evaluation accounting for the flexibility of the chain. To this end we employed cluster analysis classification of the conformations assumed by the AuΦ3 during all the trajectory times. In order to make a comparison we decided to use the same geometrical constraint previously used by Tang et al.[11]. In the following table 3.3 have been reported the cluster analysis results for the six simulations for the top five over ten generated clusters.

Times	90-100 ns	80-90 ns	70-80 ns	60-70 ns	50-60 ns	40-50 ns	30-40 ns	20-30 ns	10-20 ns	0-10 ns
Auϕ sim 1	% pop	% pop	% pop	% pop	% pop	% pop	% pop	% pop	% pop	% pop
1	18.675	12.975	9.475	11.925	11.95	15.4	48.925	22.475	5.575	4.225
2	7.8	6.825	6.5	9.75	10.2	12.65	9.9	8.875	5.125	3.5
3	7.725	6.275	6.35	6.725	8.475	9.375	7.475	5.7	4.75	3.05
4	7.7	5.125	5.825	6.175	7.675	9.05	5.725	5.625	4.3	3
5	6.9	4.875	5.725	3.8	7.675	8.9	5.525	4.8	3.85	2.9
top 5 clusters	48.8	36.075	33.875	38.375	45.975	55.375	66.3	47.475	23.6	16.675
classification	high	high	high	high	high	high	medium	high	high	high
Auϕ sim 2	% pop	% pop	% pop	% pop	% pop	% pop	% pop	% pop	% pop	% pop
1	49.35	20.8	24.475	74.425	57.775	85.85	60.325	11.35	12.825	12.6
2	30.675	13.875	16.625	18.575	11.825	6.4	25.7	9.925	9.425	4.45
3	7.75	11.25	9.5	3.475	9.05	3.9	4.45	9.15	8.325	3.575
4	3.725	10.975	9.425	2.75	8.9	3.2	2.85	6.5	7.875	3.275
5	2.725	8.425	7.7	0.3	3.55	0.275	1.9	6.425	7.25	3.25
top 5 clusters	87.775	65.325	67.725	96.475	78.65	96.15	90.475	43.35	45.7	27.15
classification	low	medium	medium	low	low	low	low	high	high	high
Auϕ sim 3	% pop	% pop	% pop	% pop	% pop	% pop	% pop	% pop	% pop	% pop
1	80.725	59.475	9.85	6.825	8.65	8.35	12.05	8.45	2.525	1.6
2	10.925	9.825	9.475	6.5	8.025	7.5	8.45	6.625	2.275	1.275
3	2.975	5.6	6.7	6.275	7.975	7.225	7.9	5.925	2.075	1.175
4	2.425	5.375	6.6	4.9	6.025	6.05	6.15	4.4	1.975	1.175
5	1.825	3.2	5.2	4.525	4.775	5.05	4.925	4.1	1.9	1.15
top 5 clusters	94.625	74.9	37.825	29.025	35.45	34.175	39.475	29.5	10.75	6.375
classification	low	medium	high	high	high	high	high	high	high	high
Times	90-100 ns	80-90 ns	70-80 ns	60-70 ns	50-60 ns	40-50 ns	30-40 ns	20-30 ns	10-20 ns	0-10 ns
Auϕ sim 4	% pop	% pop	% pop	% pop	% pop	% pop	% pop	% pop	% pop	% pop
1	17.725	27.45	59.425	32.375	34.325	11.65	24.95	21.45	3.825	2.375
2	10.6	16.55	29.65	11.275	14.025	9.225	9.925	6.8	3.5	2.025
3	10.4	7.05	6.1	10.65	9.275	7.475	7.675	5.975	3.25	1.625
4	9.05	6.75	2	8.7	5.1	7.275	5.6	5.9	3.125	1.6
5	8.3	5.325	1.6	6.075	5.025	6.75	5.025	4.575	2.95	1.55
top 5 clusters	56.075	63.125	95.175	54.3	57.625	42.375	53.175	44.7	16.65	9.175
classification	high	medium	low	medium	medium	high	high	high	high	high
Auϕ sim 5	% pop	% pop	% pop	% pop	% pop	% pop	% pop	% pop	% pop	% pop
1	56.075	25.025	33.875	32.875	22.3	9.825	4.15	21.65	19.225	1.325
2	14.225	16.275	12.275	18.475	10.825	8.425	2.925	6.85	7.425	1.2
3	8.8	12.025	10.825	10.6	6.95	6.6	2.775	4.275	5.45	1.125
4	5.425	7.125	9.075	9.25	5.5	5.1	2.75	3.65	5.2	1.05
5	5.25	5.95	7.95	4.825	4.175	4.35	2.575	3.575	4.4	1.025
top 5 clusters	79.1	53.325	56.975	61.95	49.75	34.3	15.175	40	41.7	5.725
classification	low	medium	medium	medium	high	high	high	high	hgih	high
Auϕ sim 6	% pop	% pop	% pop	% pop	% pop	% pop	% pop	% pop	% pop	% pop
1	21.325	13.225	12.65	11	7.625	29.6	11.05	28.525	26.15	8.55
2	11.175	12.95	8.55	8.55	7.025	7.45	6.975	9.8	14.925	7.025
3	7.675	12.65	7.825	7.05	6.8	6.85	5.575	8.95	6.975	6.825
4	7.45	9.05	7.3	6.175	6.7	5.9	4.7	8.325	5.55	6.35
5	5.725	8.85	6.325	4.975	5.075	4.15	4.675	7.1	5.1	5.875
top 5 clusters	53.35	56.725	42.65	37.75	33.225	53.95	32.975	47.275	58.7	34.625
classification	high	high	high	high	high	high	high	medium	high	high

Table 3.3: Cluster analysis for the six simulated systems over the whole trajectory of 100 ns.

As reported in table 3.3 the cluster analysis showed that the AuΦ3 peptide continues to assume multiple possible conformations even on the surface. The analysis reported the top clusters occupied by a little amount of population. In comparison to other inorganic binding peptides simulated by Tang et al. [11], the AuΦ3 peptide doesn't loose a great amount of configurations and consequently entropy at the interface with gold-surface. The cluster analysis matches with the presence in the sequence of both a flexible and a rigid part. The flexible part lets the chain assuming multiple adsorbed conformations on the surface till to long simulation times. The overall adsorption strength is guaranteed by the stability in time of the rigid part.
The unique binding behavior of the AuΦ3 peptide offers the possibility to use it as a bi-functional peptide in conjugation with other functional molecular entities such as cell binding ligands. A possible scheme of conjugation could be the placement of molecular motifs in the N-terminus position to promote bio-activation of the gold surface.

3.2 GRGDS-AuΦ3 and IKVAV-AuΦ3 conjugated peptides

On the basis of the previously discussed results we investigated the conformational behavior of possible conjugations of the AuΦ3 gold binding peptide with other molecular motifs, as summarized in fig.3.10. Our aim is to design sequences suitable to promote bio-activation of gold surface biomaterials for implant applications.

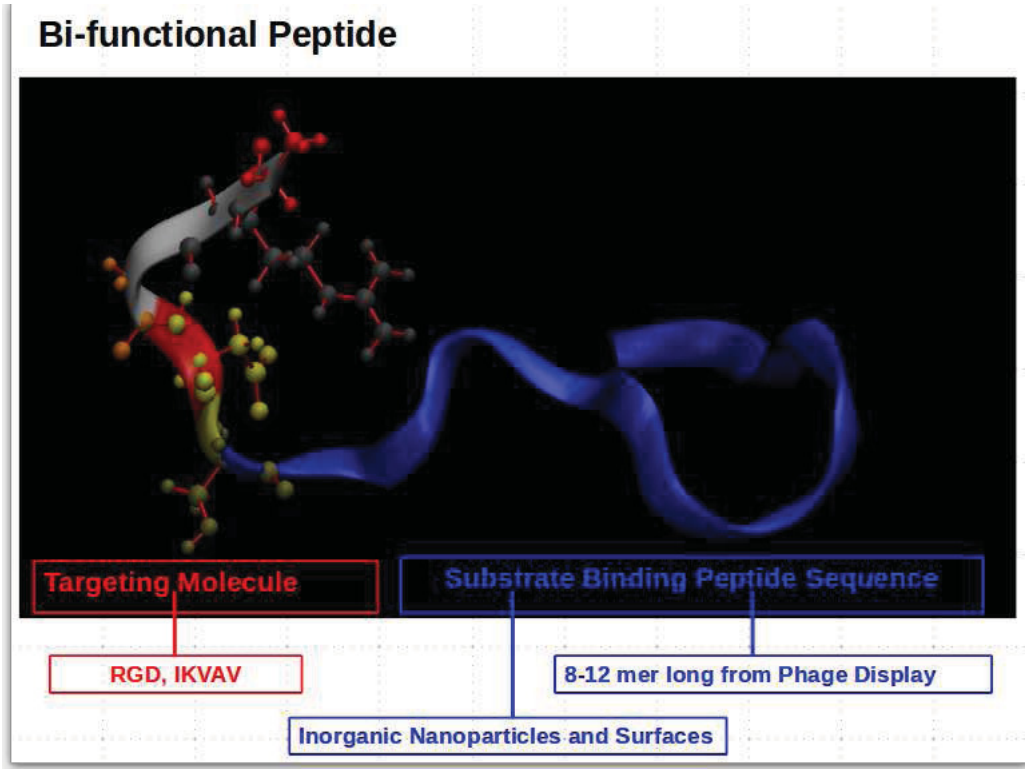

Figure 3.10: Scheme of conjugation of the Auϕ3 with molecular motifs.

Useful details can be proved studying the possible rearrangements of the longer designed chains after the conjugation. In this context how the conjugation affects the gold binding specificity of the AuΦ3 peptide is a fundamental question. Moreover, another crucial aspect is to assess if the cell binding motifs are still exposed in solution and in this way able to exert their

functionality.

We investigated the dynamics of the AuΦ3 peptide in conjugation with the cell-binding sequences composed by GRGDS (Glycine, Arginine, Glycine, Aspartic Acids and Serine) and by IKVAV (Isoleucine, Lysine, Valine, Alanine and Valine). Again we employed molecular dynamics simulations to make possible a comparison with data from the simulations of the AuΦ3 peptide.

3.2.1 Conformations above the surface

On the basis of the previous data analysis for the AuΦ3 peptide, we chose to follow the dynamics of the conjugated sequences just till 40 ns since we assessed this time is long enough to let the sequences assume stable adsorbed conformations.

Again we took the most representative conformations of the conjugated peptides during the adsorption event through the visual inspection of the trajectories. This analysis confirmed both the conjugated peptides still adsorbed on gold surface. For the conjugated peptide GRGDS-AuΦ3 we identified two groups of adsorbed configurations: one in which the whole sequence is adsorbed on gold (fig.3.11a) and another one in which both the head and tail are adsorbed and the central part is displayed in solution (fig.3.11b). In the following figures the AuΦ3 part is colored in white and reported in Ribbons representation, the GRGDS motif is blue colored and represented in CPK.

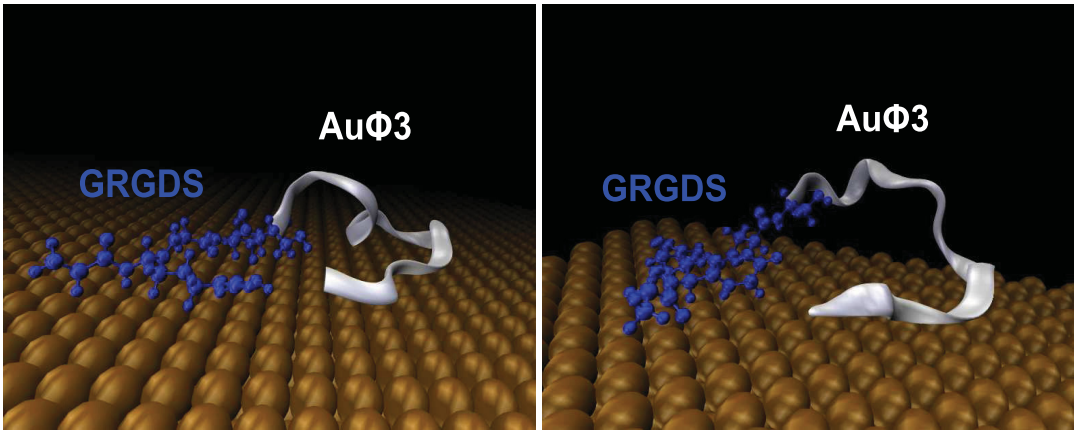

(a) (b)

Figure 3.11: Adsorbed conformations of the GRGDS-AuΦ3 peptide on gold in side view. Water molecules are omitted from clarity.

For the conjugated peptide IKVAV-AuΦ3 we assessed the majority of the conformations above the surface seems to assume a conformational behaviour

similar to the case of the AuΦ3 peptide. In the adsorbed structures there is still a part adsorbed on gold and a part displayed in solution or weakly adsorbed on gold. Two representative conformations have been reported in fig.3.12. The IKVAV sequence is red colored and represented in CPK.

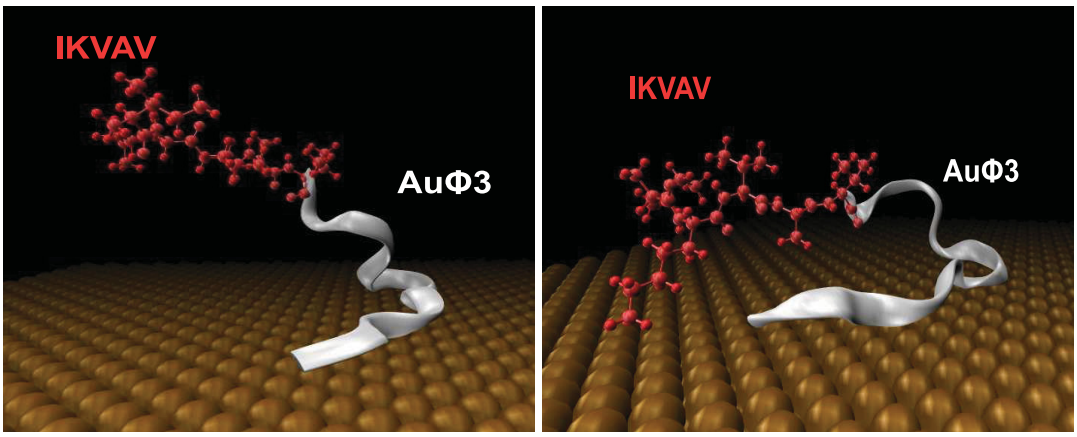

(a) (b)

Figure 3.12: Adsorbed conformations of the IKVAV-AuΦ3 peptide on gold in side view. Water molecules are omitted from clarity.

In fig.3.13 we also reported the representation of the adsorbed conjugated peptides on the gold surface in plan view.
In order to gain more accurate details about the interaction we reported the average alpha-carbons distances (figs.3.14-3.15) relative to just the adsorbed conformations at 40 ns for four systems for each conjugated sequence starting from four different initial rotations. We didn't include graphics for simulations in which the sequences didn't reach the surface.
For the sequence GRGDS-AuΦ3 the average alpha-carbons distances highlight that in three systems over four the conformations above the surface are similar. The two terminal parts are strongly adsorbed and the central part of the chain is still displayed in solution. The cell binding motif RGD seems to be strongly anchored to gold surface as expected by the presence

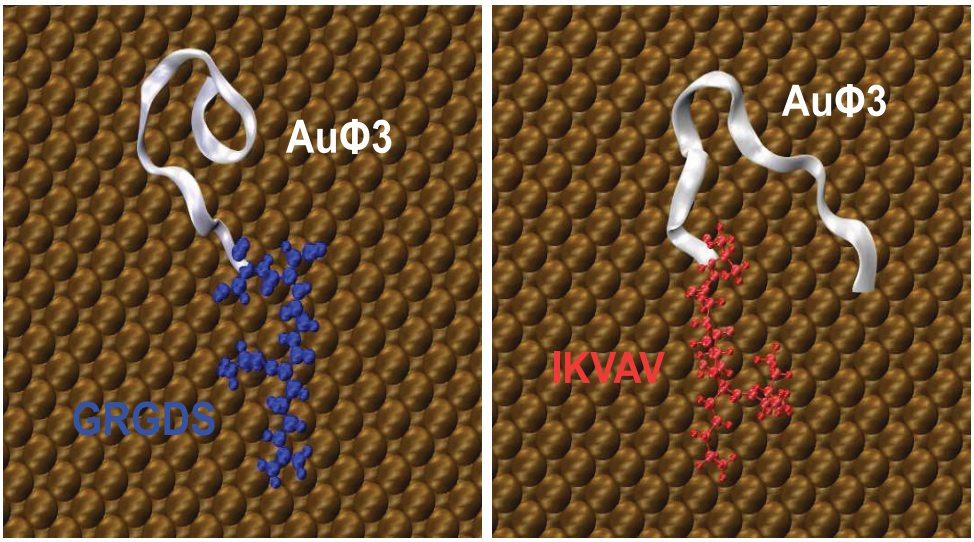

(a) (b)

Figure 3.13: Adsorbed conformations of the a) GRGDS-AuΦ3 and b) IKVAV-AuΦ3 peptides on gold in plan view. Water molecules are omitted from clarity.

in the sequence of the Arginine previously identified as a key residue in the AuΦ3 binding. In one case the sequence is completely adsorbed on gold. For the IKVAV-AuΦ3 peptide through the analysis of the average alpha-carbons distances (fig.3.15) we identified that in three systems over four the adsorbed structures show a part strongly adsorbed on gold and a part still displayed in solution. The IKVAV motif seems to be displayed in solution. In one case the sequence has both the head and the tail adsorbed and the central part exposed in solution.

Figure 3.14: Alpha-carbons distances at 40ns for GRGDS-AuΦ3 in four different simulations.

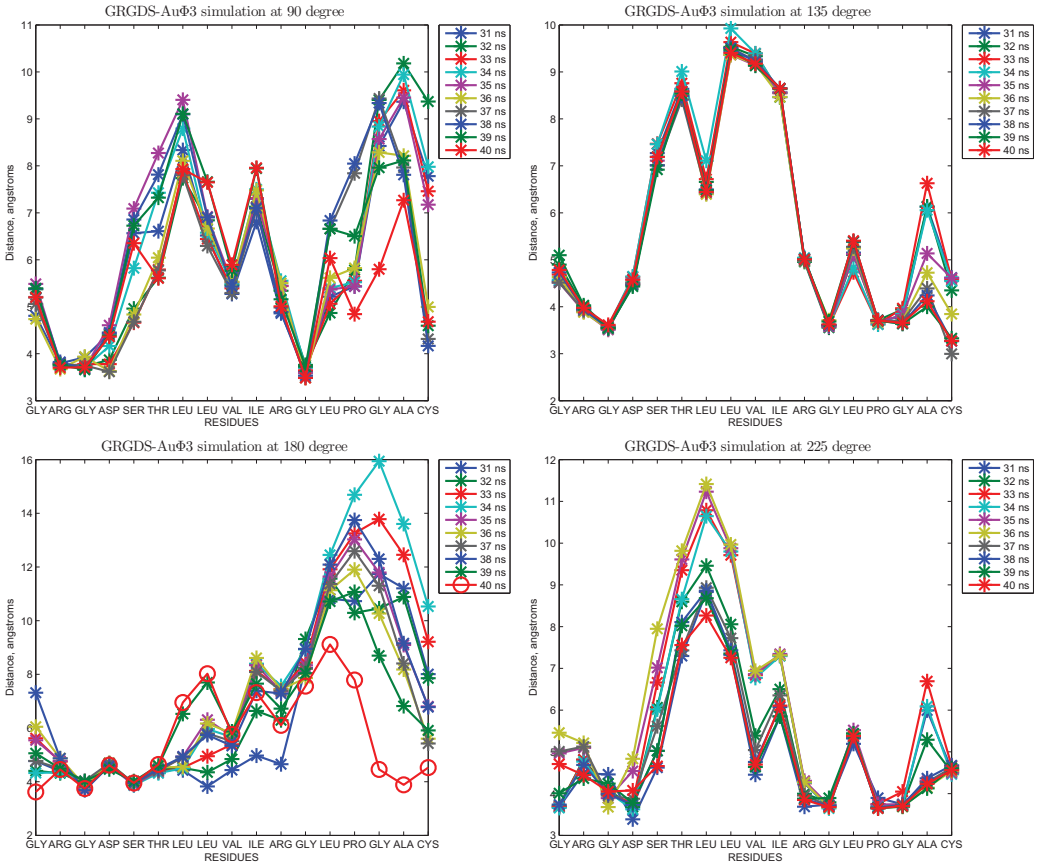

Figure 3.15: Alpha-carbons distances at 40ns for IKVAV-AuΦ3 in four different simulations.

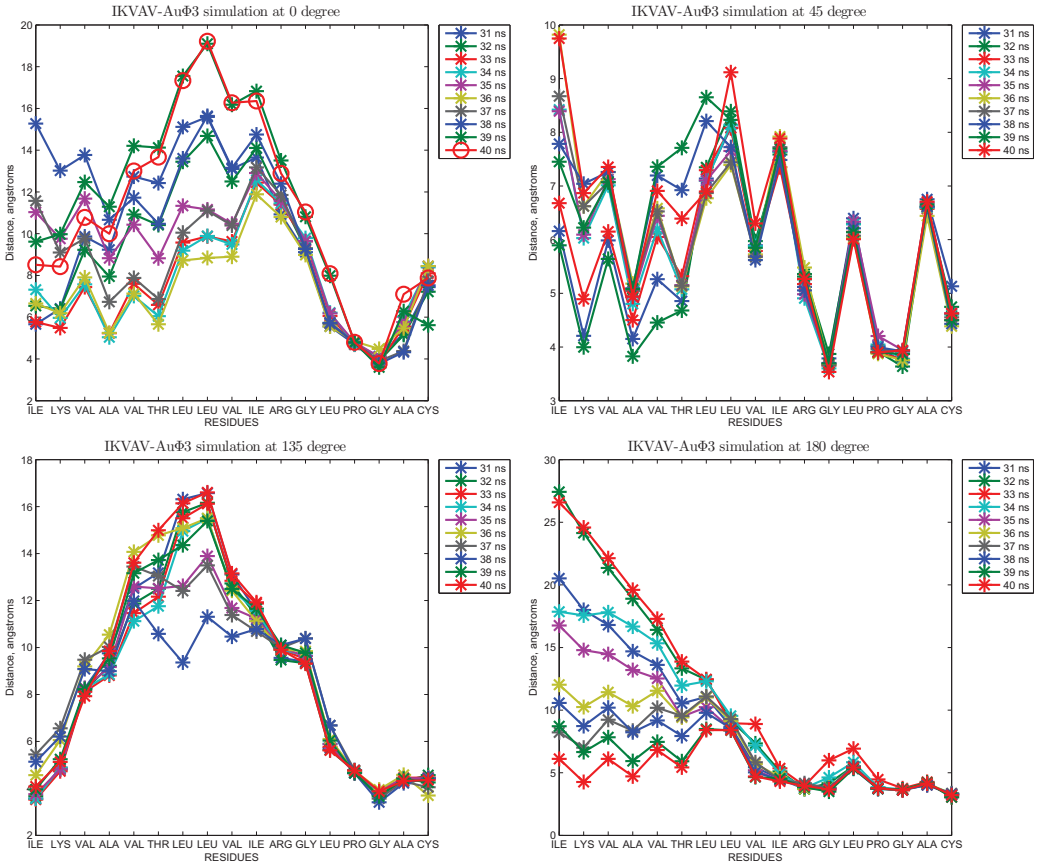

3.2.2 Adsorption maps

We reported the adsorption maps of the whole trajectory till 40 ns. We didn't include graphics for two simulations in which the sequences didn't reach the surface. For the GRGDS-AuΦ3, fig.3.16, the cell ligand sequence (GLY1, ARG2, GLY3, ASP4) appears strongly adsorbed on gold for all the simulated systems. Moreover, the adsorption of this part is stable for most of the simulated time. The part of the sequence relative to the AuΦ3 peptide is not steadily adsorbed in time. For the sequence IKVAV-AuΦ3, fig.3.17, the cell ligand motif IKVAV at 40ns is not adsorbed in three systems over four. For the AuΦ3 part, the Arginine residue is not strongly adsorbed anymore and the part mainly adsorbed is reduced to PRO14, GLY15, ALA16 and CYS17.

Figure 3.16: Adsorption maps for the sequence GRGDS-AuΦ3.

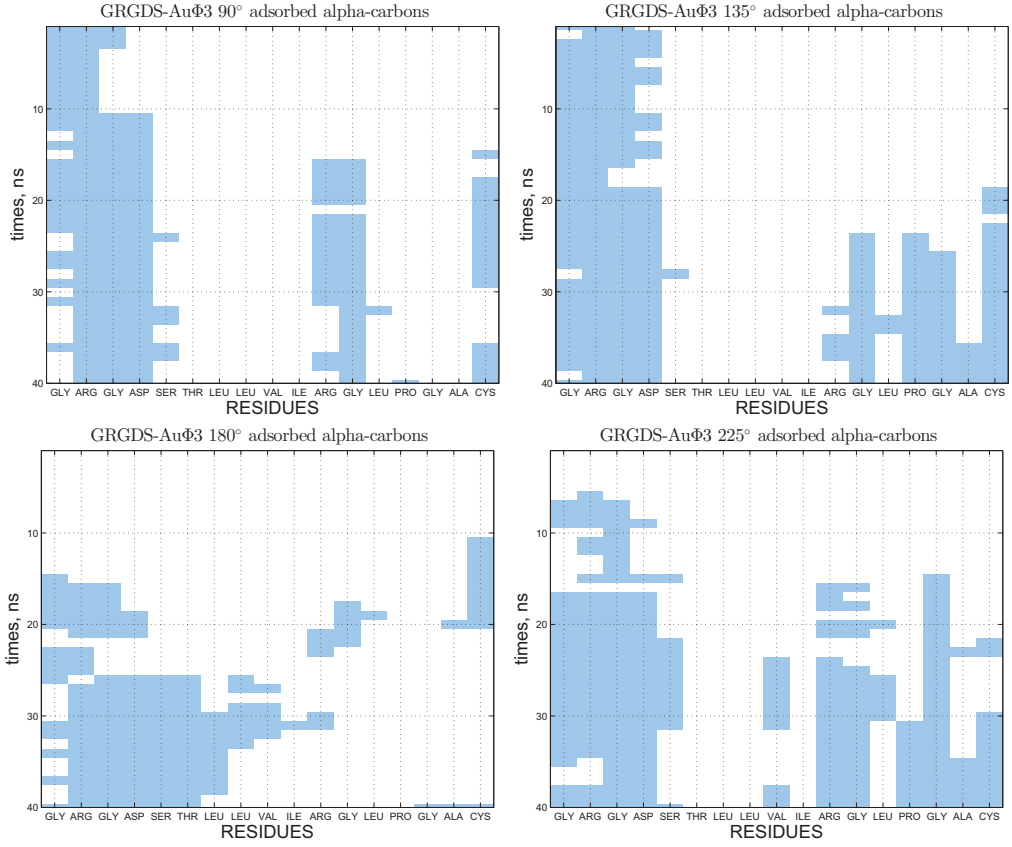

Figure 3.17: Adsorption maps for the sequence IKVAV-AuΦ3.

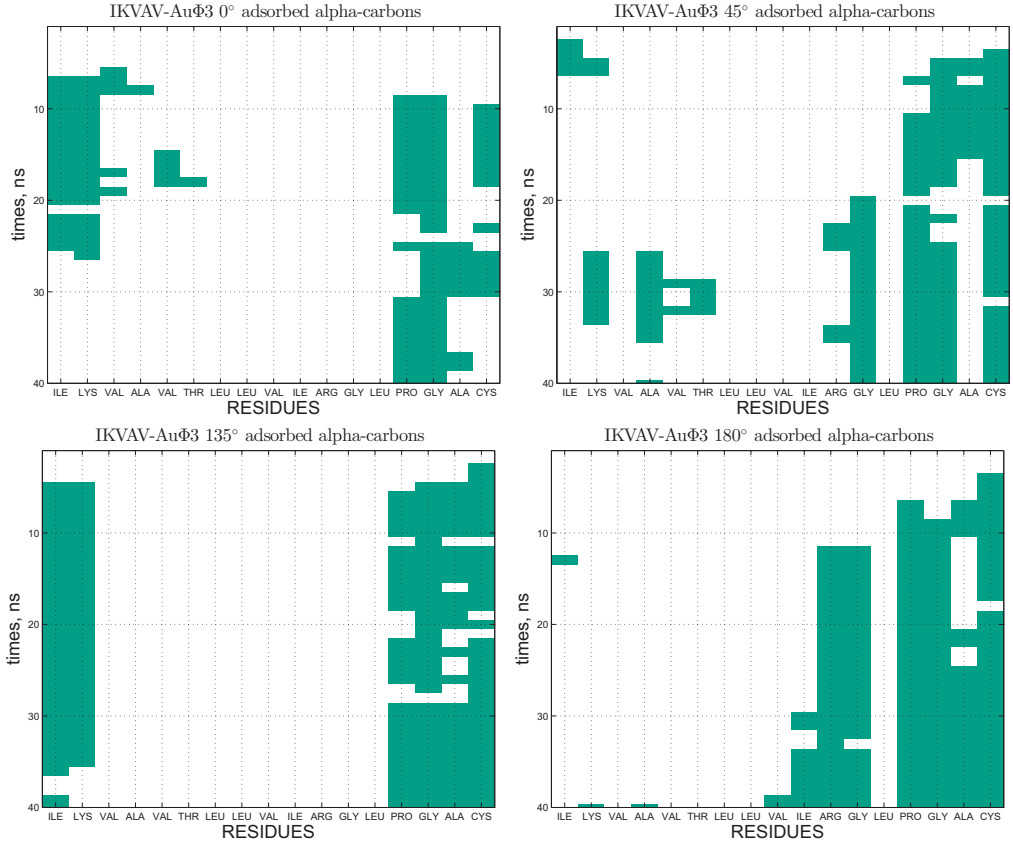

3.3 Conclusion

The adsorption of protein to a biomaterial surface strongly affects the cellular response and consequently plays a key role in the bio-compatibility of medical implants. In order to define design criteria to promote surface bio-activation of metal surfaces we employed molecular simulations of different protein sequences. First of all, we have studied the conformational behavior of a bio-combinatorially selected peptide, named AuΦ3, through molecular dynamics simulations. In a previous work, the peptide was experimentally found to exhibit a strong affinity against the gold surface both inside and outside the Phage context as proved through robust adsorption characterization. This *in silico* study has exploited different aspects of the adsorption event within an atomistic level. The binding energy computation confirmed an high affinity of the whole chain with values higher than other gold-binding peptides. The analysis of adsorption behavior in terms of the average positions of the residues in time highlights in AuΦ3 peptide a part strongly adsorbed on gold and a part preferentially displayed in solution. These unique features give the chain the possibility to explore multiple adsorbed conformations on gold surface as assessed by the cluster analysis. Moreover, a deeper investigation of the trajectories has made possible to quantify the occurrence of amino-acids to be adsorbed during the simulation time. We identified the Arginine residue to possess a crucial role in the binding event. The above discussed data outlines a complete picture of the binding behavior of the AuΦ3 peptide on gold and made possible a proposal for conjugation in the N-terminus with other molecular motifs. Furthermore we also studied the adsorption behaviour of *ad hoc* designed sequences again via molecular dynamics simulations. For the conjugated peptides with the RGD and IKVAV motifs, the analysis of the conformations above the surface and the adsorption maps has showed several differences among the sequences and in respect to the data regarding the AuΦ3 peptide. A final comparison among the sequences simu-

lated in this work in terms of the occurrence of the adsorbed amino-acids has been reported in the final fig.3.18. The bar plot evidences the IKAV-AuΦ3 sequence (turquoise bars) as the best choice to promote bio-activation of gold surface. This sequence shows two fundamental features in the adsorption on gold: on one hand it continues to display the cell binding motif in solution, on the other hand it possesses strongly anchored amino-acids on gold. For the GRGDS-AuΦ3 sequence (pale blue bars) the binding motif RGD is strongly adsorbed on gold and the amino-acids constituting the AuΦ3 part decrease their affinity in respect to the simulations of the AuΦ3 (orange bars) and IKAV-AuΦ3 sequences. The conjugation of the AuΦ3 peptide with the cell ligand sequence IKVAV offers the possibility to employ non covalent binding moieties to promote surface bio-activation of gold. This *in silico* approach could represent a tool to screen other sequences and characterize their adsorption to promote bio-activation not only of gold but also of other metal surfaces.

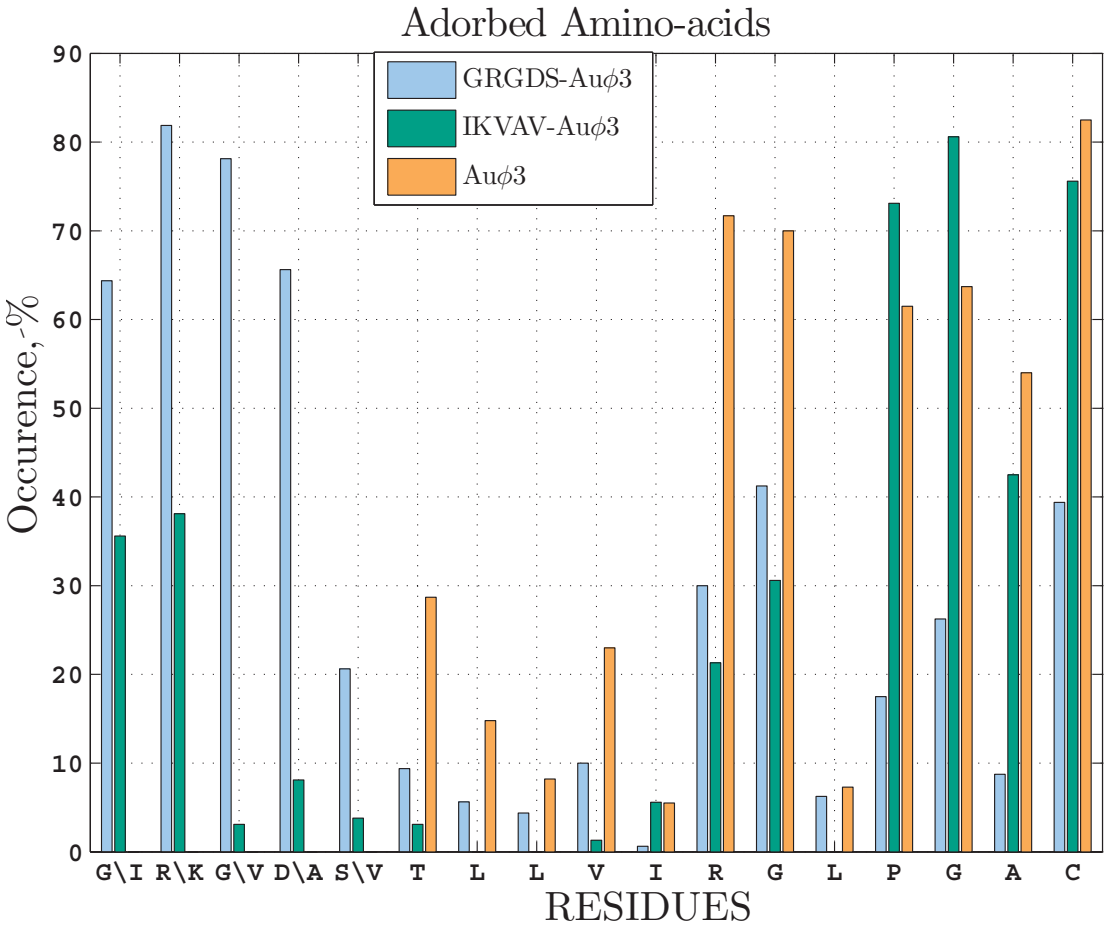

Figure 3.18: Comparison between GRGDS-AuΦ3, IKVAV-AuΦ3 and AuΦ3 peptides in terms of the occurrence of the adsorbed amino-acids.

Appendix A

Basic concepts in Molecular Dynamics

Molecular dynamics calculation computes the Newton's Second Law for every atoms of the model in order to reconstruct the time evolution of the system. The forces acting on each atom are computed as the gradient of the potential energy:

$$F_x = -\frac{\partial E}{\partial x}; F_y = -\frac{\partial E}{\partial y}; F_z = -\frac{\partial E}{\partial z}; \tag{A.1}$$

The potential energy is obtained on the basis of the molecular mechanics force field which describes equilibrium lengths (bonds, angles, diherals etc.) of each atom in the system in combination with all other atoms. The deviation from equilibrium configuration is calculated according to the potential energy expression of the force field. The energy expression consists in two contributions: the covalent one that includes bond lengths, bond angle fluctuations and dihedral angle fluctuations, and the non-covalent interactions such as electrostatic and van der Waals energies. The input informations required by the simulation are the spatial coordinates of each atom in the system at the initial time and the initial velocities. The acceleration can be obtained from the forces using Newton's Second Law. Then the changes in the velocity and position of the atom are calculated for a very short time interval, usually close to 1 fs, using numerical methods.

The time step used in the numerical integration must not exceed the vibrational frequencies in the system in order to avoid discretization. The force, acceleration and velocity are assumed to be constant during that short time. In this way, the atoms keep moving in small steps and the molecular conformations keep changing while the coordinates of each atom are saved. These trajectory data are then used to calculate different quantities during data analysis. There are three steps to solve a problem using MD methods: model building, data collection and data analysis. The quality of the computer model built determines the validity of the results: thus it is crucial to the whole study. When building a computer simulation model, researchers take into account the variables involved in the problem, the approximations used as well as the external conditions. After building a suitable model, the simulation is run for long enough to achieve an equilibrium state. Once this accomplished, the data collection period starts.

A.0.1 Energy expression of CHARMM-METAL ff

The form of the potential energy function of CHARMM-METAL ff is given by the following equation in fig.A.1. [10]

$$
\begin{aligned}
E_{pot} = & \sum_{ij \text{ bonded}} K_{r,ij}(r_{ij} - r_{0,ij})^2 + \sum_{ijk \text{ bonded}} K_{\theta,ijk}(\theta_{ijk} - \theta_{0,ijk})^2 \left(+ \sum_{ijk \text{ bonded}} K_{S,ijk}(S_{ijk} - S_{0,ijk})^2 \right) \\
& + \sum_{ijkl \text{ bonded}} V_{\phi,ijkl}[1 + \cos(n\phi_{ijkl} - \phi_{0,ijkl})] + \sum_{ijkl \text{ bonded}} K_{\chi,ijkl}[1 + \cos(n\chi_{ijkl} - \chi_{0,ijkl})] \\
& + \frac{1}{4\pi\varepsilon_0\varepsilon_r} \sum_{\substack{ij \text{ nonbonded} \\ (1,2 \text{ and } 1,3 \text{ excl})}} \frac{q_i q_j}{r_{ij}} + \sum_{\substack{ij \text{ nonbonded} \\ (1,2 \text{ and } 1,3 \text{ excl})}} \varepsilon_{ij} \left[\left(\frac{r_{0,ij}}{r_{ij}} \right)^{12} - 2 \left(\frac{r_{0,ij}}{r_{ij}} \right)^{6} \right]
\end{aligned}
$$

Figure A.1: The potetial energy expression for the CHARMM-METAL force field. From Feng et al. 2011 [10]

The first term in the energy function accounts for the bond stretches where

$K_{r,ij}$ is the bond force constant and $r_{ij} - r_{0,ij}$ is the distance from equilibrium that the atom has moved. The second term in the equation accounts for the bond angles where $K_{\theta,ijk}$ is the angle force constant and $\theta_{ijk} - \theta_{0,ijk}$ is the angle from equilibrium between 3 bonded atoms. The third term is the Urey-Bradley component (cross-term accounting for angle bending using 1,3 nonbonded interactions), where $K_{S,ijk}$ is the respective force constant and $S_{ijk} - S_{ijk}$ is the distance between the 1,3 atoms in the harmonic potential. The fourth term is for the dihedrals (a.k.a. torsion angles) where $V_{\phi,ijkl}$ is the dihedral force constant, n is the multiplicity of the function, ϕ_{ijkl} is the dihedral angle and $\phi_{0,ijkl}$ is the phase shift. The fifth term accounts for the impropers, that is out of plane bending, where $K_{\chi,ijkl}$ is the force constant and $\chi_{ijkl} - chi_{0,ijkl}$ is the out of plane angle. Nonbonded interactions between pairs of atoms are represented by the last two terms. By definition, the nonbonded forces are only applied to atom pairs separated by at least three bonds. The van Der Waals (VDW) energy is calculated with a standard 12-6 Lennard-Jones potential and the electrostatic energy with a Coulombic potential.In the 12-6 Lennard-Jones potential the ϵ_{ij} represents the equilibrium nonbond energy (obtained by geometric combination rules) and $r_{0,ij}$ the equilibrium nonbond distance (calculated by arithmetic combination rules) between two atoms i and j.

Bibliography

[1] Mehmet Sarikaya, Candan Tamerler, Alex K-Y Jen, Klaus Schulten, and Francois Baneyx. Molecular biomimetics: nanotechnology through biology. *Nature materials*, 2(9):577–585, 2003.

[2] Joseph M Slocik, Morley O Stone, and Rajesh R Naik. Synthesis of gold nanoparticles using multifunctional peptides. *Small*, 1(11):1048–1052, 2005.

[3] Candan Tamerler, Ersin Emre Oren, Memed Duman, Eswaranand Venkatasubramanian, and Mehmet Sarikaya. Adsorption kinetics of an engineered gold binding peptide by surface plasmon resonance spectroscopy and a quartz crystal microbalance. *Langmuir*, 22(18):7712–7718, 2006.

[4] Christopher R So, John L Kulp III, Ersin Emre Oren, Hadi Zareie, Candan Tamerler, John Spencer Evans, and Mehmet Sarikaya. Molecular recognition and supramolecular self-assembly of a genetically engineered gold binding peptide on au {111}. *ACS nano*, 3(6):1525–1531, 2009.

[5] Vivek P Raut, Madhuri A Agashe, Steven J Stuart, and Robert A Latour. Molecular dynamics simulations of peptide-surface interactions. *Langmuir*, 21(4):1629–1639, 2005.

[6] CP O'Brien, SJ Stuart, DA Bruce, and RA Latour. Modeling of peptide adsorption interactions with a poly (lactic acid) surface. *Langmuir*, 24(24):14115–14124, 2008.

[7] Ana Vila Verde, Jacqueline M Acres, and Janna K Maranas. Investigating the specificity of peptide adsorption on gold using molecular dynamics simulations. *Biomacromolecules*, 10(8):2118–2128, 2009.

[8] Ana Vila Verde, Peter J Beltramo, and Janna K Maranas. Adsorption of homopolypeptides on gold investigated using atomistic molecular dynamics. *Langmuir*, 27(10):5918–5926, 2011.

[9] Susana M Tomasio and Tiffany R Walsh. Modeling the binding affinity of peptides for graphitic surfaces. influences of aromatic content and interfacial shape. *The Journal of Physical Chemistry C*, 113(20):8778–8785, 2009.

[10] Jie Feng, Ras B Pandey, Rajiv J Berry, Barry L Farmer, Rajesh R Naik, and Hendrik Heinz. Adsorption mechanism of single amino acid and surfactant molecules to au {111} surfaces in aqueous solution: design rules for metal-binding molecules. *Soft Matter*, 7(5):2113–2120, 2011.

[11] Zhenghua Tang, J Pablo Palafox-Hernandez, Wing-Cheung Law, Zak E. Hughes, Mark T Swihart, Paras N Prasad, Marc R Knecht, and Tiffany R Walsh. Biomolecular recognition principles for bionanocombinatorics: An integrated approach to elucidate enthalpic and entropic factors. *ACS nano*, 7(11):9632–9646, 2013.

[12] Hendrik Heinz, RA Vaia, BL Farmer, and RR Naik. Accurate simulation of surfaces and interfaces of face-centered cubic metals using 12- 6 and 9- 6 lennard-jones potentials. *The Journal of Physical Chemistry C*, 112(44):17281–17290, 2008.

[13] Federico Iori, Rosa Di Felice, Elisa Molinari, and Stefano Corni. Golp: An atomistic force-field to describe the interaction of proteins with au (111) surfaces in water. *Journal of Computational Chemistry*, 30(9):1465–1476, 2009.

[14] F Causa, R Della Moglie, E Iaccino, S Mimmi, D Marasco, PL Scognamiglio, E Battista, C Palmieri, C Cosenza, L Sanguigno, et al. Evolutionary screening and adsorption behavior of engineered m13 bacteriophage and derived dodecapeptide for selective decoration of gold interfaces. *Journal of colloid and interface science*, 2012.

[15] Hendrik Heinz, Tzu-Jen Lin, Ratan Kishore Mishra, and Fateme S Emami. Thermodynamically consistent force fields for the assembly of inorganic, organic, and biological nanostructures: The interface force field. *Langmuir*, 29(6):1754–1765, 2013.

[16] Kin-ya Tomizaki, Shota Wakizaka, Yuichi Yamaguchi, Akitsugu Kobayashi, and Takahito Imai. Ultrathin gold nanoribbons synthesized within the interior cavity of a self-assembled peptide nanoarchitecture. *Langmuir*, 2014.

[17] Chun-Long Chen, Peijun Zhang, and Nathaniel L Rosi. A new peptide-based method for the design and synthesis of nanoparticle superstructures: construction of highly ordered gold nanoparticle double helices. *Journal of the American Chemical Society*, 130(41):13555–13557, 2008.

[18] Chun-Long Chen and Nathaniel L Rosi. Peptide-based methods for the preparation of nanostructured inorganic materials. *Angewandte Chemie International Edition*, 49(11):1924–1942, 2010.

[19] Roberto de la Rica and Hiroshi Matsui. Applications of peptide and protein-based materials in bionanotechnology. *Chemical Society Reviews*, 39(9):3499–3509, 2010.

[20] Candan Tamerler and Mehmet Sarikaya. Molecular biomimetics: genetic synthesis, assembly, and formation of materials using peptides. *MRS bulletin*, 33(05):504–512, 2008.

[21] Stanley Brown, Mehmet Sarikaya, and Erik Johnson. A genetic analysis of crystal growth. *Journal of molecular biology*, 299(3):725–735, 2000.

[22] Rajesh R Naik, Sarah J Stringer, Gunjan Agarwal, Sharon E Jones, and Morley O Stone. Biomimetic synthesis and patterning of silver nanoparticles. *Nature materials*, 1(3):169–172, 2002.

[23] Marketa Hnilova, Ersin Emre Oren, Urartu OS Seker, Brandon R Wilson, Sebastiano Collino, John S Evans, Candan Tamerler, and Mehmet Sarikaya. Effect of molecular conformations on the adsorption behavior of gold-binding peptides. *Langmuir*, 24(21):12440–12445, 2008.

[24] Beau R Peelle, Eric M Krauland, K Dane Wittrup, and Angela M Belcher. Design criteria for engineering inorganic material-specific peptides. *Langmuir*, 21(15):6929–6933, 2005.

[25] Dennis B Pacardo, Manish Sethi, Sharon E Jones, Rajesh R Naik, and Marc R Knecht. Biomimetic synthesis of pd nanocatalysts for the stille coupling reaction. *ACS nano*, 3(5):1288–1296, 2009.

[26] M Hnilova, X Liu, E Yuca, C Jia, B Wilson, AY Karatas, C Gresswell, F Ohuchi, K Kitamura, and C Tamerler. Multifunctional protein-enabled patterning on arrayed ferroelectric materials. *ACS Applied Materials & Interfaces*, 4(4):1865–1871, 2012.

[27] Anne Vallee, Vincent Humblot, and Claire-Marie Pradier. Peptide interactions with metal and oxide surfaces. *Accounts of chemical research*, 43(10):1297–1306, 2010.

[28] Haibin Chen, Xiaodi Su, Koon-Gee Neoh, and Woo-Seok Choe. Probing the interaction between peptides and metal oxides using point mutants of a tio_2-binding peptide. *Langmuir*, 24(13):6852–6857, 2008.

[29] Karsten Goede, Peter Busch, and Marius Grundmann. Binding specificity of a peptide on semiconductor surfaces. *Nano Letters*, 4(11):2115–2120, 2004.

[30] Turgay Kacar, John Ray, Mustafa Gungormus, Ersin Emre Oren, Candan Tamerler, and Mehmet Sarikaya. Quartz binding peptides as molecular linkers towards fabricating multifunctional micropatterned substrates. *Advanced Materials*, 21(3):295–299, 2009.

[31] Corrine K Thai, Haixia Dai, MSR Sastry, Mehmet Sarikaya, Daniel T Schwartz, and Francois Baneyx. Identification and characterization of cu2o-and zno-binding polypeptides by escherichia coli cell surface display: toward an understanding of metal oxide binding. *Biotechnology and bioengineering*, 87(2):129–137, 2004.

[32] Haibin Chen, Xiaodi Su, Koon-Gee Neoh, and Woo-Seok Choe. Qcm-d analysis of binding mechanism of phage particles displaying a constrained heptapeptide with specific affinity to sio_2 and tio_2. *Analytical chemistry*, 78(14):4872–4879, 2006.

[33] Urartu Ozgur Safak Seker, Vijay Kumar Sharma, Shahab Akhavan, and Hilmi Volkan Demir. Engineered peptides for nanohybrid assemblies. *Langmuir*, 2014.

[34] Marketa Hnilova, Dmitriy Khatayevich, Alisa Carlson, Ersin Emre Oren, Carolyn Gresswell, Sam Zheng, Fumio Ohuchi, Mehmet Sarikaya, and Candan Tamerler. Single-step fabrication of patterned gold film array by an engineered multi-functional peptide. *Journal of colloid and interface science*, 365(1):97–102, 2012.

[35] Ravit Nochomovitz, Moran Amit, Maayan Matmor, and Nurit Ashkenasy. Bioassisted multi-nanoparticle patterning using single-layer peptide templates. *Nanotechnology*, 21(14):145305, 2010.

[36] Marketa Hnilova, Banu Taktak Karaca, James Park, Carol Jia, Brandon R Wilson, Mehmet Sarikaya, and Candan Tamerler. Fabrication of hierarchical hybrid structures using bio-enabled layer-by-layer self-assembly. *Biotechnology and bioengineering*, 109(5):1120–1130, 2012.

[37] Maurizio Ventre, Filippo Causa, and Paolo A Netti. Determinants of cell–material crosstalk at the interface: towards engineering of cell instructive materials. *Journal of The Royal Society Interface*, 9(74):2017–2032, 2012.

[38] Candan Tamerler, Sevil Dincer, Daniel Heidel, M Hadi Zareie, and Mehmet Sarikaya. Biomimetic multifunctional molecular coatings using engineered proteins. *Progress in organic coatings*, 47(3):267–274, 2003.

[39] Dmitriy Khatayevich, Mustafa Gungormus, Hilal Yazici, Christopher So, Sibel Cetinel, Hong Ma, Alex Jen, Candan Tamerler, and Mehmet Sarikaya. Biofunctionalization of materials for implants using engineered peptides. *Acta biomaterialia*, 6(12):4634–4641, 2010.

[40] H Yazici, H Fong, B Wilson, EE Oren, FA Amos, H Zhang, JS Evans, ML Snead, M Sarikaya, and C Tamerler. Biological response on a titanium implant-grade surface functionalized with modular peptides. *Acta biomaterialia*, 9(2):5341–5352, 2013.

[41] Jungok Kim, Youngwoo Rheem, Bongyoung Yoo, Youhoon Chong, Krassimir N Bozhilov, Daehee Kim, Michael J Sadowsky, Hor-Gil Hur, and Nosang V Myung. Peptide-mediated shape-and size-tunable synthesis of gold nanostructures. *Acta biomaterialia*, 6(7):2681–2689, 2010.

[42] Yue Li, Zhenghua Tang, Paras N Prasad, Marc R Knecht, and Mark T Swihart. Peptide-mediated synthesis of gold nanoparticles: Effects of

peptide sequence and nature of binding on physicochemical properties. *Nanoscale*, 2014.

[43] Ryan Coppage, Joseph M Slocik, Beverly D Briggs, Anatoly I Frenkel, Hendrik Heinz, Rajesh R Naik, and Marc R Knecht. Crystallographic recognition controls peptide binding for bio-based nanomaterials. *Journal of the American Chemical Society*, 133(32):12346–12349, 2011.

[44] Lingyan Ruan, Hadi Ramezani-Dakhel, Chin-Yi Chiu, Enbo Zhu, Yujing Li, Hendrik Heinz, and Yu Huang. Tailoring molecular specificity toward a crystal facet: a lesson from biorecognition toward pt {111}. *Nano letters*, 13(2):840–846, 2013.

[45] Mustafa Gungormus, Hanson Fong, Il Won Kim, John Spencer Evans, Candan Tamerler, and Mehmet Sarikaya. Regulation of in vitro calcium phosphate mineralization by combinatorially selected hydroxyapatite-binding peptides. *Biomacromolecules*, 9(3):966–973, 2008.

[46] Anastasios C Manikas, Filippo Causa, Raffaella Della Moglie, and Paolo A Netti. Tuning gold nanoparticles interfaces by specific peptide interaction for surface enhanced raman spectroscopy (sers) and separation applications. *ACS applied materials & interfaces*, 5(16):7915–7922, 2013.

[47] RL Willett, KW Baldwin, KW West, and LN Pfeiffer. Differential adhesion of amino acids to inorganic surfaces. *Proceedings of the National Academy of Sciences*, 102(22):7817–7822, 2005.

[48] Martin Hoefling, Francesco Iori, Stefano Corni, and Kay-Eberhard Gottschalk. Interaction of amino acids with the au (111) surface: adsorption free energies from molecular dynamics simulations. *Langmuir*, 26(11):8347–8351, 2010.

[49] Haibin Chen, Xiaodi Su, Koon-Gee Neoh, and Woo-Seok Choe. Context-dependent adsorption behavior of cyclic and linear peptides on metal oxide surfaces. *Langmuir*, 25(3):1588–1593, 2008.

[50] Woo-Seok Choe, MSR Sastry, Corrine K Thai, Haixia Dai, Daniel T Schwartz, and François Baneyx. Conformational control of inorganic adhesion in a designer protein engineered for cuprous oxide binding. *Langmuir*, 23(23):11347–11350, 2007.

[51] Stefano Corni, Marketa Hnilova, Candan Tamerler, and Mehmet Sarikaya. Conformational behavior of genetically-engineered dodecapeptides as a determinant of binding affinity for gold. *The Journal of Physical Chemistry C*, 117(33):16990–17003, 2013.

[52] Ersin Emre Oren, Rebecca Notman, Il Won Kim, John Spencer Evans, Tiffany R Walsh, Ram Samudrala, Candan Tamerler, and Mehmet Sarikaya. Probing the molecular mechanisms of quartz-binding peptides. *Langmuir*, 26(13):11003–11009, 2010.

[53] Martin Hoefling, Susanna Monti, Stefano Corni, and Kay Eberhard Gottschalk. Interaction of β-sheet folds with a gold surface. *PloS one*, 6(6):e20925, 2011.

[54] Valeria Puddu and Carole C Perry. Peptide adsorption on silica nanoparticles: Evidence of hydrophobic interactions. *ACS nano*, 6(7):6356–6363, 2012.

[55] Siddharth V Patwardhan, Fateme S Emami, Rajiv J Berry, Sharon E Jones, Rajesh R Naik, Olivier Deschaume, Hendrik Heinz, and Carole C Perry. Chemistry of aqueous silica nanoparticle surfaces and the mechanism of selective peptide adsorption. *Journal of the American Chemical Society*, 134(14):6244–6256, 2012.

[56] Zak E Hughes, Louise B Wright, and Tiffany R Walsh. Biomolecular adsorption at aqueous silver interfaces: first-principles calculations, polarizable force-field simulations, and comparisons with gold. *Langmuir*, 29(43):13217–13229, 2013.

[57] Aerial N Camden, Stephen A Barr, and Rajiv J Berry. Simulations of peptide-graphene interactions in explicit water. *The Journal of Physical Chemistry B*, 117(37):10691–10697, 2013.

[58] Alexander D MacKerell, Donald Bashford, M Bellott, RL Dunbrack, JD Evanseck, Martin J Field, Stefan Fischer, Jiali Gao, H Guo, S a Ha, et al. All-atom empirical potential for molecular modeling and dynamics studies of proteins. *The Journal of Physical Chemistry B*, 102(18):3586–3616, 1998.

[59] Bernard R Brooks, Charles L Brooks, Alexander D MacKerell, Lennart Nilsson, Robert J Petrella, Benoît Roux, Youngdo Won, Georgios Archontis, Christian Bartels, Stefan Boresch, et al. Charmm: the biomolecular simulation program. *Journal of computational chemistry*, 30(10):1545–1614, 2009.

[60] James C Phillips, Rosemary Braun, Wei Wang, James Gumbart, Emad Tajkhorshid, Elizabeth Villa, Christophe Chipot, Robert D Skeel, Laxmikant Kale, and Klaus Schulten. Scalable molecular dynamics with namd. *Journal of computational chemistry*, 26(16):1781–1802, 2005.

[61] Rosemary Braun, Mehmet Sarikaya, and Klaus Schulten. Genetically engineered gold-binding polypeptides: structure prediction and molecular dynamics. *Journal of Biomaterials Science, Polymer Edition*, 13(7):747–757, 2002.

[62] Hendrik Heinz, Barry L Farmer, Ras B Pandey, Joseph M Slocik, Soumya S Patnaik, Ruth Pachter, and Rajesh R Naik. Nature of molec-

ular interactions of peptides with gold, palladium, and pd- au bimetal surfaces in aqueous solution. *Journal of the American Chemical Society*, 131(28):9704–9714, 2009.

[63] Hendrik Heinz. Computational screening of biomolecular adsorption and self-assembly on nanoscale surfaces. *Journal of computational chemistry*, 31(7):1564–1568, 2010.

[64] Jing Yu, Matthew L Becker, and Gustavo A Carri. The influence of amino acid sequence and functionality on the binding process of peptides onto gold surfaces. *Langmuir*, 28(2):1408–1417, 2011.

[65] Jie Feng, Joseph M Slocik, Mehmet Sarikaya, Rajesh R Naik, Barry L Farmer, and Hendrik Heinz. Influence of the shape of nanostructured metal surfaces on adsorption of single peptide molecules in aqueous solution. *Small*, 8(7):1049–1059, 2012.

[66] Jing Yu, Matthew L Becker, and Gustavo A Carri. A molecular dynamics simulation of the stability-limited growth mechanism of peptide-mediated gold-nanoparticle synthesis. *Small*, 6(20):2242–2245, 2010.

[67] William Humphrey, Andrew Dalke, and Klaus Schulten. Vmd: visual molecular dynamics. *Journal of molecular graphics*, 14(1):33–38, 1996.